MOLECULAR AND CELLULAR BIOLOGY, Dec. 2007, p. 8127–8142 Vol. 27, No. 23
0270-7306/07/$08.00+0 doi:10.1128/MCB.00912-07

RasGRF2, a Guanosine Nucleotide Exchange Factor for Ras GTPases, Participates in T-Cell Signaling Responses[▽]

Sergio Ruiz, Eugenio Santos, and Xosé R. Bustelo*

Centro de Investigación del Cáncer and Instituto de Biología Molecular y Celular del Cáncer, Consejo Superior de Investigaciones Científicas-University of Salamanca, Campus Unamuno, E-37007 Salamanca, Spain

Received 23 May 2007/Returned for modification 6 July 2007/Accepted 18 September 2007

The Ras pathway is critical for the development and function of T lymphocytes. The stimulation of this GTPase in T cells occurs primarily through the Vav1- and phospholipase C-γ1-dependent activation of RasGRP1, a diacylglycerol-responsive Ras GDP/GTP exchange factor. Here, we show that a second exchange factor, RasGRF2, also participates in T-cell signaling. RasGRF2 is expressed in T cells, translocates to immune synapses, activates Ras, and stimulates the transcriptional factor NF-AT (nuclear factor of activated T cells) through Ras- and phospholipase C-γ1-dependent routes. T-cell receptor-, Vav1-, and Ca^{2+}-elicited pathways synergize with RasGRF2 for NF-AT stimulation. The analysis of RasGRF2-deficient mice indicates that this protein is required for the induction of bona fide NF-AT targets such as the cytokines tumor necrosis factor alpha and interleukin 2, while it plays minor roles in Ras activation itself. The comparison of lymphocytes from *Vav1*$^{-/-}$, *Rasgrf2*$^{-/-}$, and *Vav1*$^{-/-}$; *Rasgrf2*$^{-/-}$ mice demonstrates that the RasGRF2 pathway cooperates with the Vav1/RasGRP1 route in the blasting transformation and proliferation of mature T cells. These results identify RasGRF2 as an additional component of the signaling machinery involved in T-cell receptor- and NF-AT-mediated immune responses.

T-cell receptor (TCR) engagement triggers a complex series of intracellular signaling steps that are essential for proper T-cell development and function (35). This cascade of signaling events is initiated by the antigen-dependent activation of protein tyrosine kinases that, upon phosphorylation of downstream elements such as Vav1, phospholipase C-γ1 (PLC-γ1), and phosphatidylinositol 3-kinase promote the activation of multiple biological responses (35). Current evidence indicates that one of the critical downstream routes targeted by both the pre-TCR and the mature TCR is the Ras pathway. Thus, it has been shown that Ras GTPases and specific Ras-dependent effectors such as c-Raf1, MEK, ERK1, and ERK2 are important for the passage of immature T cells through the β checkpoint, the allelic exclusion of *tcr*β genes, the positive selection step, and the final thymocyte commitment towards the mature $CD4^+$ lineage (1, 29). The Ras pathway also plays roles in mature lymphocytes, being important for bypassing the anergy state (28, 57), for promoting the induction of the CD69 marker (19), and for activating the nuclear factor of activated T cells (NF-AT) (55), a transcriptional factor crucial for T-cell proliferation (38).

In order to fulfill these functions, the three members of the Ras family (H-Ras, K-Ras, and N-Ras) fluctuate rapidly and transiently between an inactive, GDP-bound state and an active, GTP-bound conformation (15). Under conditions of cell stimulation, the transition from the GDP- to the GTP-bound state is mediated by enzymes referred to as guanosine nucleotide exchange factors (GEFs), GDP-releasing proteins (GRPs), or GDP-releasing factors (GRFs) (42). The reverse transition is modulated by GTPase-activating proteins (GAPs), a group of enzymes promoting hydrolysis of the bound GTP molecules at the end of the stimulation cycle (46). After an initial point of controversy that postulated that the activation of Ras in T cells was due to a diacylglycerol (DAG)- and protein kinase C (PKC)-dependent inhibition of a GAP activity (32), more-recent results have shown that the surge in the levels of GTP-Ras originated upon pre-TCR and TCR engagement relies primarily on the activation of Ras GEFs (32). However, unlike other cell types that use primarily the Sos GEF family (42), the main exchange factor involved in the TCR-mediated activation of Ras is RasGRP1 (23), a DAG-dependent exchange factor (24, 51). The activation of RasGRP1 requires a complex array of signaling events, including the TCR-dependent tyrosine phosphorylation of the Rho/Rac GEF Vav1, the subsequent increase in DAG levels by the Vav1-dependent stimulation of PLC-γ1, and the final activation of RasGRP1 by DAG molecules (11, 43, 61). The Vav1/PLC-γ1 pathway enhances RasGRP1 activity further by favoring the F-actin-dependent translocation of RasGRP1 to the plasma membrane and by promoting an additional DAG/PKC-dependent phosphorylation step (11, 44). In addition, to promote the canonical GDP/GTP exchange on Ras GTPases, Ras GRP1 also seems to contribute to the concentration of the stimulation of the Ras pathway in specific subcellular compartments. For example, it has been shown that, depending on the extracellular stimuli, RasGRP1 can activate Ras proteins in the plasma membrane (20, 40) and/or the Golgi apparatus (6, 10, 20, 41). Although this regulatory aspect is still controversial in lymphocytes (4, 11, 61), recent results performed with primary thymocytes have shown that the specific activation of Ras in the Golgi apparatus and plasma membrane is important for the positive and negative selection steps, respectively (20). Despite

* Corresponding author. Mailing address: Centro de Investigación del Cáncer and Instituto de Biología Molecular y Celular del Cáncer, CSIC-University of Salamanca, Campus Unamuno, E-37007 Salamanca, Spain. Phone: 34-923-294802. Fax: 34-923-294743. E-mail: xbustelo@usal.es.

▽ Published ahead of print on 8 October 2007.

the marginal role of Sos1 during TCR signaling, recent results have shown that its activity may be useful to amplify the initial pool of activated Ras induced by RasGRP1 (45). However, it cannot be ruled out at this moment that Sos1 or Sos2 may play important roles in the signaling pathways of other T-cell receptors such as integrins or cytokine receptors.

The RasGRF family represents an additional group of Ras GEFs (42). The two known members of this family, RasGRF1 and RasGRF2 (25, 39, 48), harbor a complex array of structural domains (see Fig. 5A), including two pleckstrin homology (PH) regions, a coiled-coil motif, a Ca^{2+}/calmodulin binding ilimaquinone (IQ) domain, a Dbl homology (DH) region acting both as a homodimerization region and as a catalyzer of the GDP/GTP exchange on the GTPase Rac1 (2, 26), a Ras exchange motif, and the prototypical Cdc25 Ras exchange domain common to all Ras GEFs (42). To date, the characterization of these GEFs has been mostly focused on neuronal processes due to their prevalent expression in brain. Consistent with this role, signaling experiments and the analysis of *Rasgrf1*$^{-/-}$ and *Rasgrf2*$^{-/-}$ mice have indicated that these GEFs play important roles in the signaling of glutamate receptors and in long-term memory potentiation (8, 36, 50). Despite this evidence, the detection of rat *rasgrf2* transcripts outside the brain and the serious defects observed in the pancreatic β cells of *Rasgrf1*$^{-/-}$ mice suggest that these proteins may have roles outside the nervous system (25, 30). In this work, we examined this possibility in the case of TCR-triggered signaling events.

MATERIALS AND METHODS

Animals. *Rasgrf2*$^{-/-}$ mice were described previously (27). *Vav1*$^{-/-}$ mice were generously provided by V. Tybulewicz (NIMR, London, United Kingdom) (52). *Vav1*$^{-/-}$; *Rasgrf2*$^{-/-}$ mice were generated by crossing the above mouse strains. All mice used in this work were homogenized in the B10.BR genetic background. Unless otherwise indicated, six- to eight-week-old animals were used in all the experiments.

Antibodies. Antibodies to small epitope tags (hemagglutinin [HA] and FLAG) and green fluorescent protein (GFP) were obtained from Covance. The antibodies to RasGRF family members and to phosphotyrosine residues were obtained from Santa Cruz Biotechnology. A pan-specific anti-Ras antibody was purchased from Upstate Biotechnology. Anti-tubulin antibodies were from Oncogene. The rabbit antibodies to the phosphorylated Y174 residue of Vav1 and the Vav1 DH (catalog no. 301-5) have been generated in our laboratory and described previously (37). The rabbit antibodies to either total extracellular signal-related kinase (ERK) or the phosphorylated Thr202 and Tyr204 residues of ERK1/ERK2 were obtained from Cell Signaling. The rabbit antibodies specific to either total PLC-γ1 or the phosphorylated Y783 residue of PLC-γ1 were both obtained from BD Transduction Laboratories. Horseradish peroxidase-conjugated secondary antibodies to rabbit and mouse immunoglobulin G (IgG) were obtained from GE Healthcare. The Alexa 594-labeled secondary antibodies to either rabbit or mouse IgG were from Invitrogen.

Plasmids. Plasmids encoding wild-type human Vav1 (pJC11), human H-Ras(S17N) (pXRB20), and the rat RasGRF1 Cdc25 region (pXRB28) have been previously described by us (9). The mammalian expression vector pMEX has been referenced before (9). pCEV-RasGRF1 (rat RasGRF1) and pcDNA3-FLAG-RasGRF2 (mouse RasGRF2) were kindly provided by L. Feig (Tufts University School of Medicine, Boston, MA) and M. Moran (University of Toronto, Ontario, Canada), respectively. The plasmid encoding the HA-tagged isoform 1 of Sos1 (pCEFL-KZ-HA-hSos1 Isof1) was obtained from J. M. Rojas (Instituto Carlos III, Madrid, Spain) and described previously (11). pCXN2-FLAG-RasGRP1, pCEV-RasGRF1ΔPH1, pCEV-RasGRF1-ΔDH, pCEV-RasGRF1ΔPH2, pCEFL-HA-H-Ras, pCEFL-HA-K-Ras, pCEFL-HA-N-Ras, pCEFL-HA-ERK1, pCEFL-FLAG, and pGEX-RafRBD (encoding the glutathione *S*-transferase [GST] protein fused to the Ras binding domain of c-Raf1) were obtained from P. Crespo (CSIC-University of Cantabria, Santander, Spain). The pEGFP-CD3ξ plasmid was provided by B. Alarcón (Centro de Biología Molecular, CSIC, Madrid, Spain). pCI*neo*-PLC-γ1 (a mammalian expression vector encoding an HA-tagged version of bovine PLC-γ1) was obtained from E. Bonvini (NIH, Bethesda, MD). The pNF-AT*luc* reporter plasmid was obtained from G. Crabtree (Stanford University Medical School, Stanford, CA). pRL-SV40 was from Promega. Expression vectors encoding H-Ras(C181S, C184S) and M1-H-Ras(C181S, C184S) have been described previously (11). Plasmids encoding the red fluorescence protein (RFP) (pDsRed-C1) and the enhanced GFP (EGFP) (pEGFP-C1) were obtained from Clontech. For the generation of the EGFP-RasGRF2-encoding vector (pSRM4), the full-length mouse *rasgrf2* cDNA was excised from pcDNA3-FLAG-RasGRF2 by KpnI/ApaI digestion and ligated into the KpnI/ApaI-linearized pEGFP-C1 plasmid (BD Biosciences/Clontech Laboratories). To create the mammalian expression vector encoding the RasGRF2(L263Q) point mutant (pSRM6), we used a QuikChange site-directed mutagenesis kit (Stratagene) with the pcDNA3-FLAG-RasGRF2 plasmid as template and the 5′-GCTGAGTACGTCCAGCAGCAACACATCCTTGTCAACAAC-3′ (forward) and 5′-GTTGTTGACAAGGATGTGTTGCTGCTGGACGTA-3′ (reverse) primers. To generate the mammalian expression vector encoding a RasGRF1 protein with a frame-shift mutation on its IQ domain (pSRM12), we mutated the original pCEV-RasGRF1 to introduce and remove single nucleotides at the beginning and at the end of the IQ domain, respectively. To this end, we used a QuikChange kit in two sequential mutagenesis steps: in the first round, we used the 5′-GAGGATGAGGACAGTACATCAAGAAAATTA-3′ (forward) and 5′-TAATTTTCTTGATGTACTGTCCTCATCCTC-3′ (reverse) primers. This single point mutant was used as template in the second PCR round utilizing the 5′-GGAAGAACATCATCCCAGGACTACATCCGG-3′ (forward) and 5′-CCGGATGTAGTCCTGGGATGATGTTCTTCC-3′ (reverse) primers. To generate the PLC-γ1(Y783F) point mutant (pSRM15), we used a QuikChange kit with the primers 5′-CAACCCTGGCTTCTTTGTGGAGGCGAACCC-3′ (forward) and 5′-GGGTTCGCCTCCACAAAGAAGCCAGGGTTG-3′ (reverse). For the generation of the vector expressing the FLAG-RasGRF1ΔCdc25 protein (pSRM8), a PCR-generated *rasgrf1* cDNA fragment amplified from pCEV-RasGRF1 was digested using BamHI and BglII and ligated into the BamHI/BglII-linearized pCEV-RasGRF1 (pSRM2). After this cloning step, a BamHI/XbaI fragment containing the *rasgrf1*Δ*cdc25* cDNA was excised from pSRM2 and ligated into the BglII/XbaI-linearized pCEFL-FLAG vector to generate the final pSRM8 vector. For the generation of the expression plasmid encoding the EGFP-RasGRF1 protein (pSRM30), the full-length *rasgrf1* cDNA was excised from pSRM2 by digestion with BamHI and NotI and ligated into the BamHI/NotI-linearized pEGFP-C1. For the generation of the vector expressing FLAG-RasGRF2ΔIQ (pSRM34), a PCR fragment was amplified by PCR from pcDNA3-FLAG-RasGRF2, digested with BamHI and XhoI, and ligated into BamHI/XhoI-linearized pcDNA3-FLAG-RasGRF2. The *rasgrf2*ΔIQ cDNA was excised from this plasmid by digestion with KpnI and ApaI and ligated into the KpnI/ApaI-linearized pEGFP-C1 to generate the mammalian expression vector encoding the EGFP-tagged version of RasGRF2ΔIQ (pSRM36). For the generation of the FLAG-RasGRF2ΔCdc25-encoding vector (pSRM33), a PCR fragment was amplified from pcDNA3-FLAG-RasGRF2, digested with EcoRI and XhoI, and ligated into the EcoRI/XhoI-linearized pcDNA3-FLAG-RasGRF2 plasmid to generate the pSRM32 vector. Then, the *rasgrf2*Δ*cdc25* cDNA was excised from pSRM32 with KpnI and ApaI and ligated into the KpnI/ApaI-linearized pEGFP-C1 vector. To generate the EGFP-Vav2-encoding vector (pAA7), the full-length mouse *vav2* cDNA was amplified by PCR from pXRB138 (47), digested with EcoRI, and ligated into EcoRI-linearized pEGFP-C1. All constructs generated were subjected to automatic sequencing to rule out the presence of extra mutations. All PCR and sequencing primers are available upon request.

Purification of splenic T cells. To isolate total RNA from $CD4^+$ or $CD8^+$ T cells, splenocytes were obtained by tissue disruption, treated with 0.17 M NH_4Cl to eliminate erythrocytes, washed twice in phosphate-buffered saline solution (PBS), and stained with fluorescein isothiocyanate (FITC)-labeled anti-CD4 (BD Biosciences) and allophycocyanin (APC)-labeled anti-CD8 (BD Biosciences) for 30 min. After extensive washes in PBS, cellular suspensions were sorted in FACSArea apparatus (BD Biosciences). A minimum of 5×10^5 $CD4^+$ or $CD8^+$ cells was isolated. Cells negative for CD4 and CD8 expression were also separated and referred to as "non-T cells." For detecting the phosphorylation levels of ERK in vivo, splenocytes were obtained by mechanical disruption as above and then T cells were purified via a high-affinity negative selection method using T-cell enrichment columns (R&D Systems). T-cell-enriched fractions were washed, resuspended in RPMI without serum, and stimulated by incubation with the indicated amounts of an Armenian hamster anti-CD3 antibody (BD Biosciences) for 10 min on ice followed by cross-linking with 50 μg of a goat antibody to Armenian hamster IgGs (Jackson Immunoresearch) at 37°C for 3 min. Flow cytometry analysis indicated the percentage of T cells in these fractions was always higher than 90%.

Isolation of RNAs. Total RNAs from cell populations were isolated using an RNeasy Mini kit (QIAGEN) as indicated by the manufacturer. Total RNAs from mouse tissues and human Jurkat cells were obtained using the Trizol reagent (Invitrogen) according to the manufacturer's recommendations. In all cases, the integrity and concentration of the RNAs obtained were evaluated using an Agilent 2100 bioanalyzer.

RT-PCR. In these experiments, the reverse transcription (RT) step was performed using a SuperScript first-strand synthesis system for RT-PCR (Invitrogen). Primers for the amplification of the mouse *rasgrf2* cDNA were 5′-GTGAGGGCCAGAAAGCTGTCTTTGACGTCT-3′ (forward) and 5′-TCGGCTACCTGTCCTCCAGGCCTGCCGATT-3′ (reverse). Primers for the amplification of the mouse *rasgrf1* cDNA were 5′-CAGAAAGCCATCCCGCTTAAC-3′ (forward) and 5′-GTCCTTGATCAGGTTTGCAATC-3′ (reverse). Primers for the amplification of the human *rasgrf2* cDNA were 5′-AGGCCCTATGGGAACTGTCTC-3′ (forward) and 5′-CTGCTGCTCTCTCCCTGGAG-3′ (reverse). Primers for the amplification of the human *rasgrf1* cDNA were 5′-CTGCCTCCACAACTACAATGC-3′ (forward) and 5′-GAAACTGGCGAATGTCTCGGA-3′ (reverse). The amplification of the *actin* cDNA fragments was used as an internal control of the RT-PCR using oligonucleotide primers 5′-GTGACGAGGCCCAGAGCAAGAG-3′ (forward) and 5′-AGGGGCCGGACTCATCGTACTC-3′ (reverse). As an additional positive control, we amplified the rat *rasgrf1* and mouse *rasgrf2* cDNA by PCR using as templates the mammalian expression vectors pCEV-RasGRF1 and pcDNA3-FLAG-RasGRF2, respectively. The rat cDNA sequences are highly similar to their mouse counterparts and, therefore, can be amplified using the primers designed for the mouse *rasgrf* family cDNAs. As negative control, we used samples in which the RT step was bypassed.

Cell culture and DNA transfections. The T-cell Jurkat and lymphoblastoid B-cell Raji cell lines were both cultured at 37°C in a humidified 5% CO_2 atmosphere in RPMI 1640 supplemented with 10% fetal calf serum plus 100 units/ml of penicillin and streptomycin. For DNA transfections, 2×10^7 exponentially growing Jurkat cells were collected, resuspended in 200 μl of RPMI 1640, and electroporated with the indicated plasmids using a Gene Pulser II apparatus (250 V, 950 μF; Bio-Rad). 293T cells were cultured in Dulbecco's minimal essential medium supplemented with 10% calf serum and transfected using the calcium phosphate precipitation method (53). When needed, transfections were supplemented with an empty vector (pMEX) to normalize the total amount of DNA introduced in the cells. All tissue culture reagents were from Gibco/Invitrogen. LAT- and PLC-γ1-deficient Jurkat cells have been described previously (34, 59).

Immunoblotting. Equal amounts of tissue or cell lysates were diluted 1:1 with sodium dodecyl sulfate-polyacrylamide gel electrophoresis (SDS-PAGE) sample buffer and boiled for 10 min. Lysates were then separated electrophoretically and transferred onto nitrocellulose filters (Schleicher and Schuell). Membranes were incubated with the appropriate antibodies, and immunoreactive bands were visualized using a standard chemiluminescence detection system (Pierce).

Ras activation assays. Twenty-four hours after electroporation, Jurkat cells were stimulated with either anti-CD3 antibodies (0.5 μg/ml; Dako) or ionomycin (0.25 μg/ml; Sigma/Aldrich) for 5 min and lysed, and the levels of GTP-bound Ras were determined using pulldowns with a bacterially expressed GST-RBD fusion protein as previously described (61).

Conjugate formation and time-lapse fluorescence microscopy. Jurkat cells were transiently transfected by electroporation with the appropriate expression vectors 16 h before being used. Raji cells were loaded at 37 °C for 20 min with the fluorescent cell tracker 7-amino-4-chloromethylcoumarin (CMAC) (10 μM; Molecular Probes/Invitrogen) in serum-free media, washed, resuspended in RPMI 1640 supplemented with 10% fetal calf serum, and preloaded with staphylococcal enterotoxin E (1 μg/ml; Toxin Technology) for 2 h at 37°C. To allow the formation of T-cell/B-cell conjugates, the transfected Jurkat cells (2×10^6 cells) were mixed with an equal number of those Raji cells in a final volume of 40 μl and conjugates were formed by cell sedimentation during 30 min at 37°C. Then, conjugates were resuspended and allowed to settle for 15 min at room temperature onto poly-L-lysine-coated coverslips (EMD Biosciences/Calbiochem). Attached cells were fixed for 15 min in 4% formaldehyde in PBS and then permeabilized for 10 min in 1% Triton X-100 in PBS. Cells were stained with the indicated antibodies followed by Alexa 594-labeled anti-rabbit or anti-mouse IgG antibodies (Molecular Probes/Invitrogen). For time-lapse microscopy, glass-bottom culture plates (Mat-Tek) were coated with fibronectin (20 μg/ml) for 20 h at 4°C and then saturated with Hanks' balanced salt solution (HBSS) (Gibco/Invitrogen) containing 1% bovine serum albumin for 30 min at 37°C. Plates were washed with HBSS and placed onto the microscope stage. Transiently transfected Jurkat cells (15×10^4) resuspended in HBSS were allowed to attach in those fibronectin-coated plates for 30 min at 37°C. Then, CMAC-labeled Raji cells (1×10^5) loaded with staphylococcal enterotoxin E were added onto the plate-attached Jurkat cells and conjugate formation was monitored by collecting pictures of cultures every minute using an inverted Axiovert 2000 microscope. Images were processed with the MetaMorph software (version 6.1; Molecular Devices) to generate the final movies.

NF-AT luciferase assays. Exponentially growing Jurkat cells were electroporated with 10 μg of a firefly luciferase reporter plasmid containing NF-AT sites (pNF-AT-*luc*), 5 ng of a plasmid (pRL-SV40) encoding the *Renilla* luciferase, and the appropriate combination of expression plasmids (10 μg each). The total amount of transfected DNA was kept constant in all transfections by supplementing them with an empty pMEX vector. Forty-eight hours after transfection, cells were either left resting or stimulated with anti-CD3 antibodies (0.5 μg/ml) or ionomycin (1 μg/ml) for 8 h. When appropriate, cells were preincubated before stimulation with 1,2-bis(*o*-aminophenoxy)ethane-N,N,N′,N′-tetraacetic acid (BAPTA) (50 μM; EMD Biosciences/Calbiochem) for 1 h. Cells were then harvested and luciferase activities determined using a dual luciferase reporter system (Promega), according to the supplier's instructions. The values of firefly luciferase activity obtained in the different samples were always normalized taking into account the activity of the *Renilla* luciferase obtained in each sample. To confirm comparable expression of proteins in all samples, aliquots of lysates were subjected to SDS-PAGE and immunoblotted with the indicated antibodies. Each experiment shown has been repeated in at least three independent transfections.

Immunoprecipitations. In the case of lymphocytes, Jurkat cells were electroporated with 10 μg of each mammalian expression vector. After 36 h, cells were lysed in 20 mM Tris-HCl (pH 7.5), 150 mM NaCl, 1 mM EDTA, 1 mM EGTA, 1% Triton X-100, 1 mM NaF (Sigma/Aldrich), 100 μM Na_2VO_4 (Sigma/Aldrich), and the Complete protease inhibitor cocktail (Roche Applied Science) and the cleared cell extracts were immunoprecipitated depending on the experiment with either anti-HA (to detect the phosphorylation levels of PLC-γ1) or anti-FLAG (to detect RasGRF2/PLC-γ1 association) antibodies for 2 h at 4°C. Immunoprecipitates were then collected using Gammabind Sepharose beads (GE Healthcare), washed thrice, and boiled in 1× SDS-PAGE sample buffer. Eluted proteins were separated electrophoretically and analyzed by immunoblot analysis with the indicated antibodies. 293T cells were transfected using 7 μg of either pcDNA3-FLAG-RasGRF2 or pCXN2-FLAG-RasGRP1 alone or in combination with 7 μg of pCI*neo*-PLC-γ1 (see above). After 36 h, cells were lysed and processed for immunoprecipitation as indicated above.

Flow cytometry analysis. Single-cell suspensions were prepared by homogenization of the indicated tissues with the aid of 50-μm filters (Falcon). After erythrocyte lysis by hypotonic shock in 0.17 M NH_4Cl, thymic and spleen lymphocyte populations were stained with antibodies to surface markers using appropriate combinations of FITC-labeled anti-CD4 and anti-CD44 antibodies, peridinin chlorophyll protein-labeled anti-CD4, anti-CD25, and anti-CD69 antibodies, and APC-labeled anti-CD4, anti-CD8, and anti-B220 antibodies (BD Biosciences). The expression of interleukin 2 (IL-2) and tumor necrosis factor alpha (TNF-α) was measured intracellularly. To this end, splenocytes were treated with brefeldin A (10 μg/ml; Sigma/Aldrich) to block the secretory machinery and stimulated with either anti-CD3 (2 μg/ml; BD Biosciences) or anti-CD3 (1 μg/ml) plus anti-CD28 (0.5 μg/ml; BD Biosciences) for 6 h. Cells were then collected, washed, stained with FITC-labeled anti-CD4 and APC-labeled anti-CD8 antibodies, fixed in 4% formaldehyde in 1.4× PBS, permeabilized with 0.5% saponin, and stained with phycoerythrin-labeled anti-IL-2 and anti-TNF-α antibodies (BD Biosciences). Flow cytometry analyses were conducted using a FACSCalibur system (BD Biosciences) and analyzed using the Cell Quest (BD Biosciences), Paint-a-Gate, and WinMDI 2.8 software packages.

CFSE staining. Splenocytes were washed twice in PBS, resuspended at 20×10^6 cells/ml, and diluted with an equal volume of CFSE (2 μM; Invitrogen/Molecular Probes) in PBS. After 5 min under rotation, the cell labeling was stopped by the addition of fetal calf serum to the cell suspensions and subsequent washes in PBS. CFSE-labeled splenocytes were stimulated with either anti-CD3 (1 μg/ml) or a combination of anti-CD3 (0.5 μg/ml) plus anti-CD28 (0.2 μg/ml) antibodies. At the indicated times, cells were harvested, stained with either peridinin chlorophyll protein-labeled anti-CD4 or APC-labeled anti-CD8 antibodies, and analyzed by flow cytometry.

RESULTS

RasGRF2 is expressed in T lymphocytes. Previous studies have shown that, unlike the *rasgrf1* locus, the *rasgrf2* gene is expressed in different rat tissues such as brain, kidney, liver, lung, pancreas, and spleen (25). To investigate whether *rasgrf2*

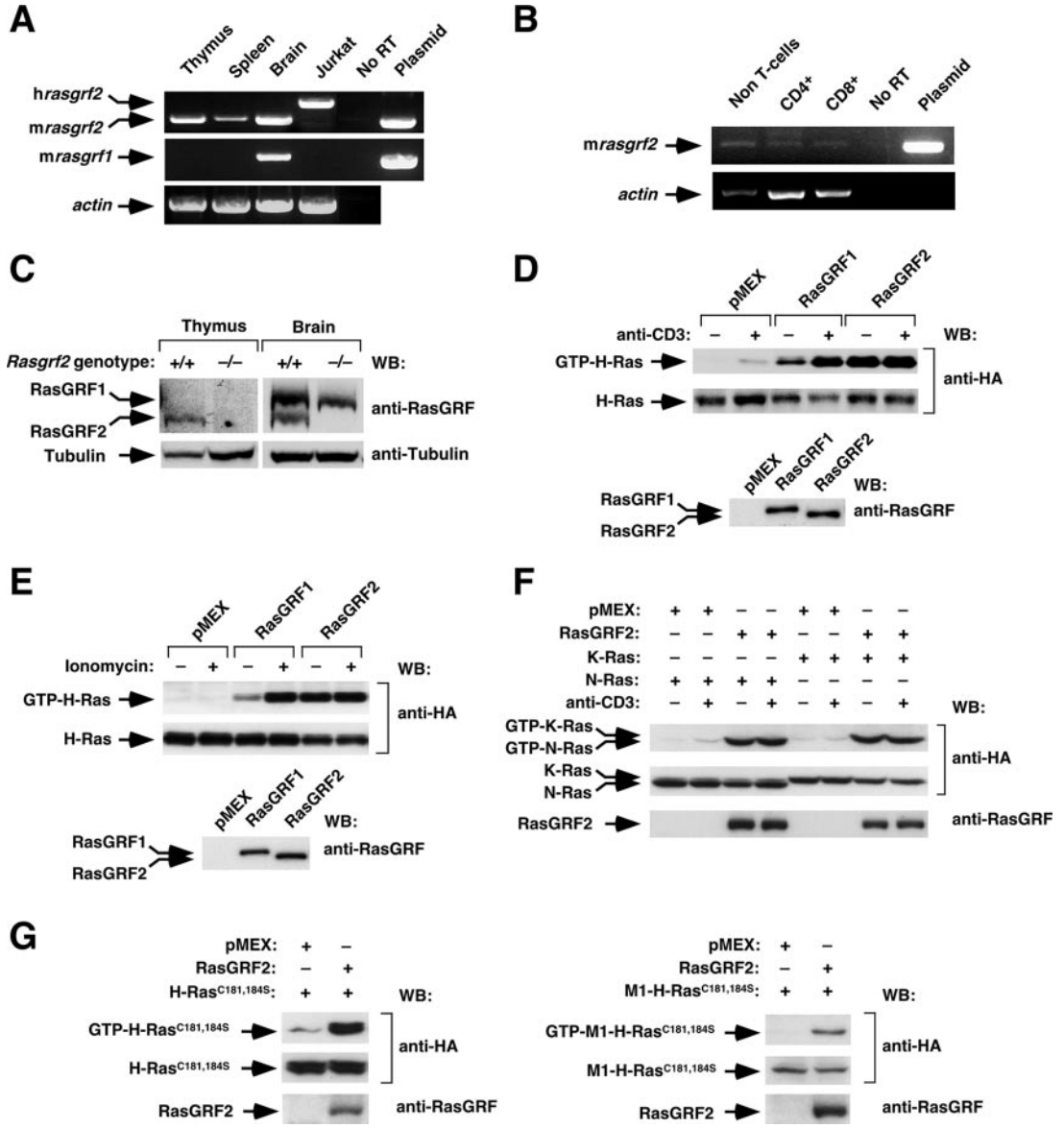

FIG. 1. RasGRF2 is expressed and active in T-cell populations. (A and B) RT-PCR analysis to detect the indicated genes in tissues (A), Jurkat cells (A), and sorted splenic lymphocytes (B). As a positive control, we included amplifications using template vectors containing mouse *rasgrf2* (top in panels A and B) and rat *rasgrf1* (middle in panel A) cDNAs. No RT, PCR analysis with RT conducted in the absence of the first step of cDNA synthesis. (C) Immunoblot analysis of the expression of RasGRF proteins in the mouse tissues of the indicated genotypes. (D to F) Jurkat cells expressing the indicated proteins (top) were either left unstimulated (−) or stimulated (+) with anti-CD3 (D and F) or ionomycin (E). After lysis, cellular extracts were subjected to GST-RBD pulldown experiments to reveal the populations of GTP-bound HA-H-Ras (D and E), HA-N-Ras (F), and HA-K-Ras (F) present in each sample (upper panels). In parallel, aliquots of the same total cellular lysates were immunoblotted with the indicated antibodies (right) to determine the expression levels of Ras (middle panels) and RasGRF proteins (lower panels). (G) Jurkat cells expressing the indicated combinations of proteins (top) were subjected to pulldown experiments as indicated above to reveal the level of GTP loading of H-Ras(C181S, C184S) (upper panel on the left) and M1-H-Ras(C181S, C184S) (upper panel on the right) induced by RasGRF2. Aliquots of the same total cellular lysates were immunoblotted with the indicated antibodies to determine the expression levels of Ras (middle panels) and RasGRF proteins (bottom panels). WB, Western blot.

was also present in the lymphoid compartment, we first analyzed the expression of the two *rasgrf* family members in cDNA samples obtained from different tissues and cells using RT-PCR assays. These analyses indicated that *rasgrf2* was indeed expressed in the thymus, the Jurkat T-cell line, and, previously described in rat tissues (25), in the spleen (Fig. 1A). *rasgrf2* transcripts were also detected in splenic $CD4^+$ and $CD8^+$ T cells as well as in other hematopoietic populations composed mostly of splenic $B220^+$ B cells (Fig. 1B). In contrast, the *rasgrf1* mRNA was only found in brain-derived cDNAs (Fig. 1A). To further verify the expression of the *rasgrf2* gene in lymphoid organs at the protein level, we subjected tissue extracts obtained from either $Rasgrf2^{+/+}$ or $Rasgrf2^{-/-}$ mice to immunoblot analysis using a pan-specific antibody to RasGRF family

members. As shown in Fig. 1C, the 135-kDa RasGRF2 protein was detected in both the brain and thymus of wild-type animals. As expected, this protein was missing in the tissue lysates obtained from *Rasgrf2*$^{-/-}$ mice (Fig. 1C). In contrast, the 140-kDa RasGRF1 protein was only detected in brain samples regardless of the mouse genotype tested in the experiments (Fig. 1C). These results raised the possibility that RasGRF2 could have specific functional roles in T lymphocytes.

Participation of RasGRF2 in T-cell signaling events. We investigated next the possible implication of RasGRF2 in signaling events triggered by the TCR. Since T cells express high levels of other Ras-specific GEFs such as Sos1 and RasGRP1 that could obscure the visualization of RasGRF-specific responses, we resorted to overexpression experiments in Jurkat cells to investigate the connection of RasGRF2 with upstream TCR signals and, subsequently, its possible implication in downstream biological responses. RasGRF1 was also included in these experiments in order to obtain information about the regulatory and signaling specificities of the two RasGRF family members. Given that RasGRFs contain a Ca^{2+}/calmodulin-binding IQ motif (42), we decided to analyze the ability of these two exchange factors to promote activation of H-Ras protein in the context of both TCR cross-linking and induction of intracellular Ca^{2+} fluxes. To this end, Jurkat cells expressing the indicated combinations of ectopic proteins were left unstimulated or, alternatively, stimulated with anti-CD3 antibodies or ionomycin, a Ca^{2+} ionophore. The levels of GTP-bound H-Ras were then determined in cell lysates by pulldown analyses. Consistent with previous results in nonhematopoietic cells (21), these experiments indicated that RasGRF2 displayed a constitutive GDP/GTP exchange activity that promoted high levels of GTP-bound H-Ras even in the absence of cell stimulation (Fig. 1D and E). Such behavior was not conserved in the case of RasGRF1, since this protein promoted maximal levels of H-Ras activation only in stimulated cells (Fig. 1D and E). Previous studies have shown both inducible and constitutive activity of RasGRF1 towards Ras in nonhematopoietic cells (2, 13, 60). Constitutive activation of two additional Ras family members, the GTPases K-Ras and N-Ras, was also observed upon overexpression of RasGRF2 in Jurkat cells (Fig. 1F).

Unlike K-Ras, H-Ras and N-Ras can become activated not only at the plasma membrane but also in endomembrane structures such as the endoplasmic reticulum and the Golgi apparatus (3, 6, 7, 10, 14, 41). To verify whether RasGRF2 could activate Ras proteins outside the plasma membrane, we performed additional pulldown experiments with two H-Ras mutant proteins, H-Ras(C181S, C184S) and M1-H-Ras(C181S, C184S). H-Ras(C181S, C184S) is a palmitoylation-deficient protein that localizes in both the endoplasmic reticulum and the Golgi apparatus. M1-H-Ras(C181S, C184S) is fused to the cytoplasmic tail of the first transmembrane domain of the avian bronchitis virus M protein and, as a consequence, is localized exclusively in the endoplasmic reticulum (10, 14). As shown in Fig. 1G, these two mutant H-Ras proteins were also activated by RasGRF2, suggesting that this GEF can stimulate Ras proteins in the plasma membrane and endomembrane regions. This result is in full agreement with previous results by us and Crespo's group using nonhematopoietic cells (3, 10).

Next, we analyzed whether RasGRF2 could translocate to the immune synapse (54). To approach this issue, we used both time-lapse and standard confocal microscopy to track down the subcellular localization of EGFP-tagged RasGRF2 during the formation of the immune synapse between Jurkat cells and superantigen-loaded Raji cells. In nonengaged Jurkat cells, the EGFP-RasGRF2 fusion protein was evenly distributed in the cytosol (Fig. 2A). However, this protein translocated to the immune synapse right after the initial contact of the Jurkat with the superantigen-loaded B cell (Fig. 2A). Similar results were obtained with EGFP-RasGRF1 (S. Ruiz and X. R. Bustelo, unpublished data). To verify that this translocation was a specific event, we incorporated two controls in these experiments. First, we demonstrated that a nonchimeric EGFP could not translocate to the immune synapse under the same experimental conditions used for the EGFP-RasGRF2 fusion protein (Fig. 2B). Secondly, by coexpressing a nonchimeric RFP with the EGFP-RasGRF2, we could demonstrate that the translocation step was an exclusive property of the EGFP-RasGRF2 protein (Fig. 2B). Interestingly, the distribution of EGFP-
RasGRF2 and EGFP-RasGRF1 proteins at the immune synapse was more disperse than that observed with the TCR- and plasma membrane-associated CD3ξ protein (Ruiz and Bustelo, unpublished). EGFP-RasGRFs also showed in general a more-dispersed distribution in the synapse than those displayed by other well-known components of the immune synapse, such as phosphorylated Vav1 (Fig. 2B). The translocation of EGFP-RasGRF2 to the immune synapse also occurred in the case of RasGRF2 mutant proteins lacking either the IQ or the Cdc25 domains (Ruiz and Bustelo, unpublished), indicating that the tethering of this exchange factor to the plasma membrane was independent of the possible interaction of Ca^{2+} with the IQ region or of the accumulation of GDP-bound Ras GTPases at the immune synapse. This is in contrast to the behavior of RasGRF2 in nonhematopoietic cells, where a Ca^{2+}-dependent mechanism of membrane translocation has been reported (25).

To complete the initial characterization of the implication of RasGRF2 in TCR signals, we analyzed the influence of RasGRF family proteins on the activation of NF-AT, a TCR-activated transcriptional factor crucial for both T-cell activation and differentiation (38). As a positive control we used Vav1, a signal transduction molecule that potently activates the NF-AT pathway (56). These experiments indicated that RasGRF proteins and Vav1 induced high levels of NF-AT activity already in nonstimulated cells (Fig. 3A). Such activation was further enhanced upon stimulation of Jurkat cells with either anti-CD3 antibodies or ionomycin (Fig. 3A). Whereas the levels of NF-AT activation obtained by anti-CD3 antibodies were similar in the case of RasGRF family proteins and Vav1, we observed that RasGRF1 and RasGRF2 differed significantly in the level of stimulation achieved with ionomycin. Thus, whereas RasGRF2 and Vav1 showed an enhancement of NF-AT activity levels upon the ionomycin treatment similar to that observed with the CD3 cross-linking, RasGRF1 responded more potently to the ionomycin stimulation (Fig. 3A). This differential behavior cannot be attributed solely to different levels of activation of Ras, because RasGRF1 and RasGRF2 activate H-Ras to similar levels upon activation of Jurkat cells with any of those two stimuli (Fig. 1D and E). To rule out

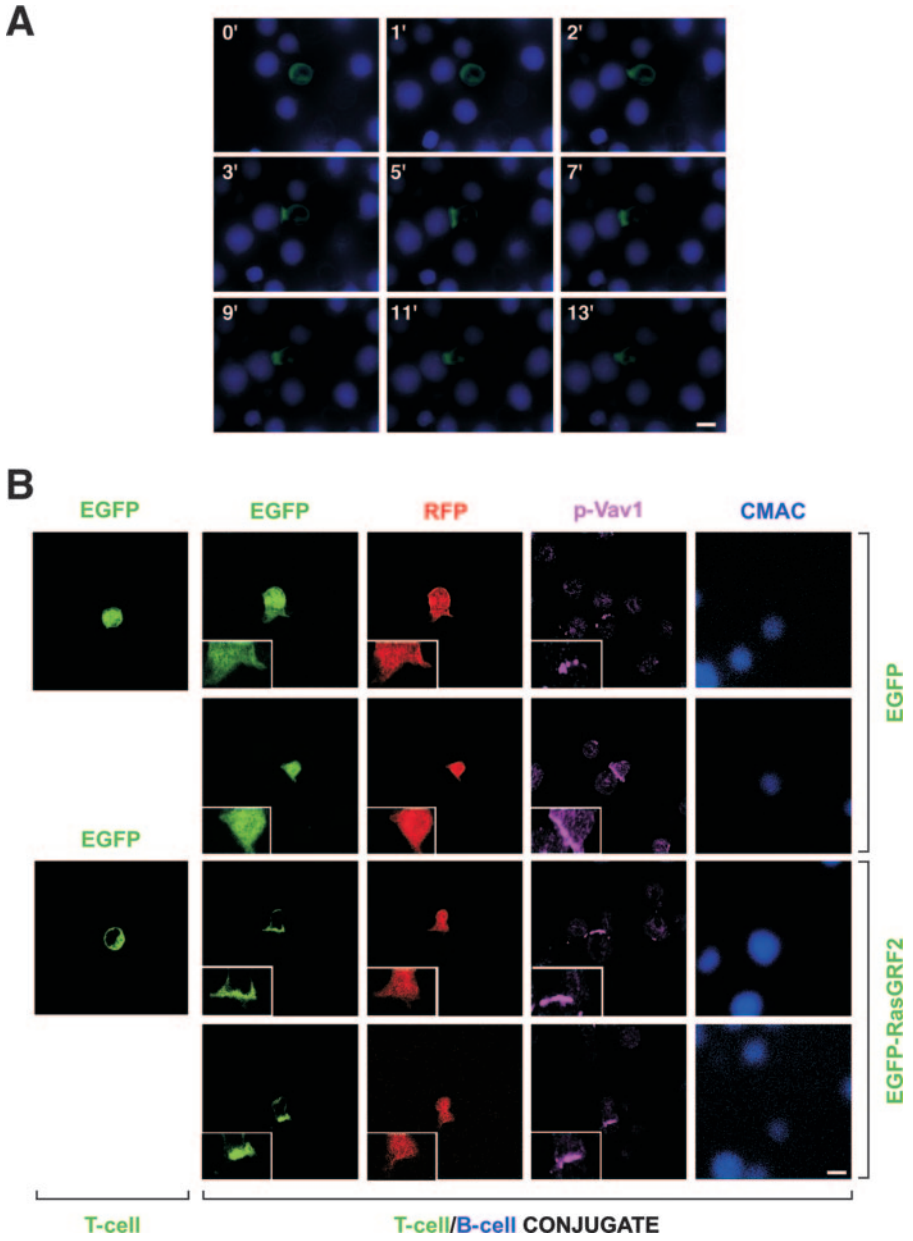

FIG. 2. Translocation of RasGRF proteins to the immune synapse. (A) Jurkat cells transiently expressing EGFP-RasGRF2 were subjected to conjugate formation with CMAC-labeled Raji B cells and analyzed by time-lapse fluorescence microscopy. Time after conjugation is shown in the upper left corner of each panel. (B) Jurkat cells expressing RFP with either EGFP (two upper rows) or EGFP-RasGRF2 (two lower rows) were left unconjugated (left column) or incubated with CMAC-labeled, superantigen-loaded Raji cells to allow the formation of T-cell/B-cell conjugates (the rest of the columns). Conjugates were then plated onto coverslips, fixed, stained with antibodies to Vav1 phosphorylated on tyrosine 174, and analyzed by confocal fluorescence microscopy. Images show in green, red, and purple the localization of EGFP (first and second columns from the left), the nonchimeric RFP (third panel from the left), and phospho-Vav1 (p-Vav1, fourth panel from the left), respectively. B cells are shown in blue (column on the right). Scale bar, 10 μm.

that the activation of NF-AT was a nonspecific consequence of the overexpression of either Ras or Rac1 exchange factors, we compared the activation of NF-AT induced by Vav1 and RasGRF2 with that obtained upon transfection of other Ras-specific (RasGRP1), Rho/Rac-specific (Vav2), and bifunctional (Sos1) exchange factors. These experiments indicated that RasGRP1, Sos1, and as previously described (5, 22), Vav2 could not activate NF-AT (Fig. 3B). Taken together, these results indicate that RasGRF2 can activate constitutively the Ras pathway in T cells and that it participates in the signal transduction pathway that mediates the activation of NF-AT. More importantly, the activation of NF-AT is an intrinsic property of RasGRF2 that is not shared by other Ras superfamily GEFs. As in the case of Vav1, RasGRF proteins cooperate with TCR- and Ca^{2+}-dependent routes to induce maximal levels of NF-AT activity.

RasGRF proteins synergize with the Vav1 pathway in NF-AT activation. It is known that the stimulation of NF-AT

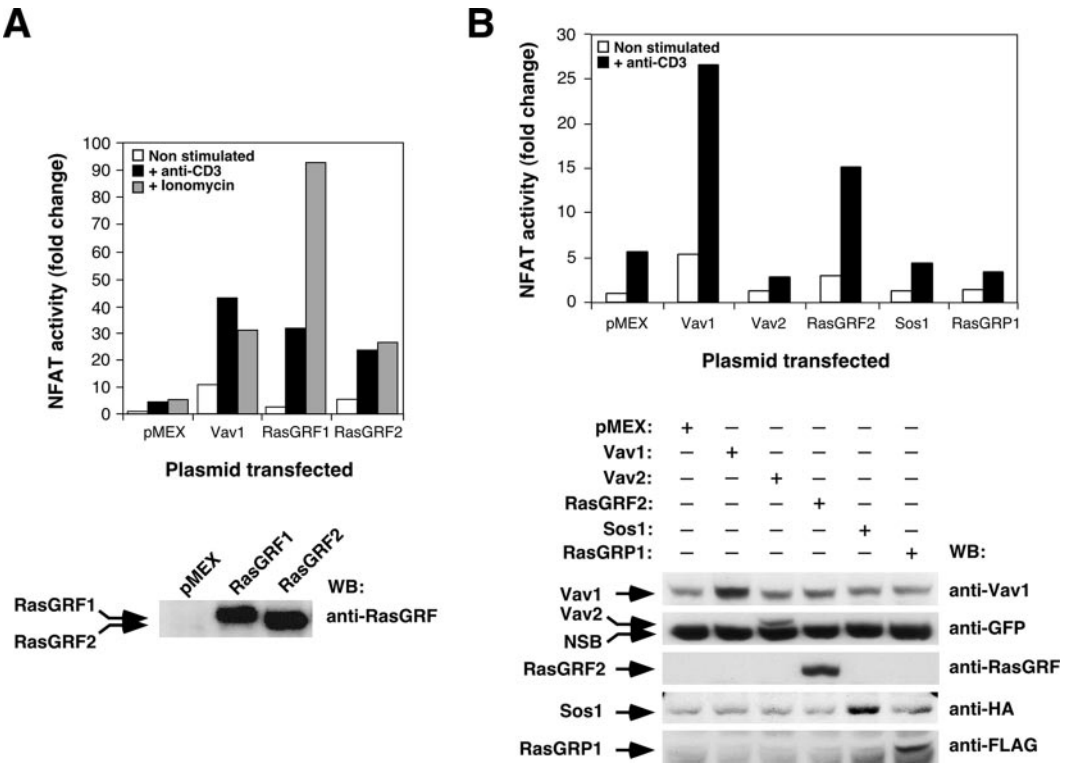

FIG. 3. RasGRF proteins stimulate NF-AT. Jurkat cells electroporated with the pNF-AT*luc* reporter plasmid and expressing the indicated proteins were stimulated as indicated. After stimulation, NF-AT activities were determined using a luciferase assay. Results are expressed as change relative to the NF-AT activity present in nonstimulated cells that had been transfected with an empty vector (pMEX). A representative experiment performed in triplicate is shown in each panel. The expression of proteins used in this experiment was determined by Western blot. Similar results were obtained in three independent experiments. NSB, nonspecific band recognized by the anti-GFP antibodies in Jurkat cells; WB, Western blot.

requires a complex concatenation of signaling events engaged by the parallel stimulation of Ras and calcineurin, a Ca^{2+}-dependent phosphatase (55). Because of this, optimal activation of NF-AT can be obtained by combining the expression of an oncogenic Ras version with either constitutively active calcineurin mutants or with stimulation of cells with Ca^{2+} ionophores. Alternatively, it can be induced by the expression of molecules that, like Vav1, promote the simultaneous activation of Ras and Ca^{2+} (56). To get further insight into the mechanism by which RasGRF proteins promote NF-AT activity, we first evaluated the effect of the Vav1 and the Ras pathways on the RasGRF-triggered NF-AT activity by using luciferase reporter experiments. As shown in Fig. 4A, both the basal and the anti-CD3-mediated stimulation of NF-AT increased upon the coexpression of RasGRF proteins with Vav1. In agreement with the known inhibition of Vav1-dependent stimulation of NF-AT by dominant-negative Ras (S17N mutant) (56), the synergistic response obtained by the coexpression of Vav1 and RasGRF2 was totally abolished by Ras(S17N) (Fig. 4A). This dominant-negative mutant also inhibited the NF-AT stimulation induced by RasGRF proteins alone (Ruiz and Bustelo, unpublished), indicating that this signaling response requires the Ras pathway. However, pulldown experiments indicated that the coexpression of Vav1 induced only minor changes in the GDP/GTP exchange activity of RasGRF proteins in vivo (Fig. 4B), suggesting that the enhanced NF-AT response found in cells coexpressing Vav1 and RasGRF2 probably entailed the engagement of additional signaling pathways. This lack of synergism between Vav1 and RasGRF2 in Ras activation is in contrast to the cooperative response found between Vav1 and RasGRP1 in the same experimental system (61). Vav1 alone did not trigger detectable GDP/GTP exchange on ectopically expressed H-Ras proteins (Fig. 4B) because, in order to do so, it requires RasGRP1 coexpression (61). These results indicate that RasGRF proteins act in parallel to Vav1 or, alternatively, utilize some of the downstream elements used by Vav1 to promote NF-AT stimulation. In addition, they suggest that the synergistic effect of Vav1 and RasGRF2 in NF-AT activity requires both the Ras pathway and additional signal transduction routes.

RasGRF proteins require Ras-dependent and -independent functions to promote NF-AT activation. We next used a collection of RasGRF1 and RasGRF2 mutants already available in our laboratory to investigate the role of its structural domains in the regulation of NF-AT activity (Fig. 5A). Using GST-RBD pulldown experiments, we observed that the only RasGRF1 domain required for the activation of H-Ras was the catalytic Cdc25 region (Fig. 5B). Accordingly, the single expression of this domain in Jurkat cells promoted levels of GTP loading of H-Ras similar to those observed with the wild-type full-length protein (Fig. 5B, protein 7). Conversely, the deletion of the Cdc25 GEF domain renders RasGRF1 proteins

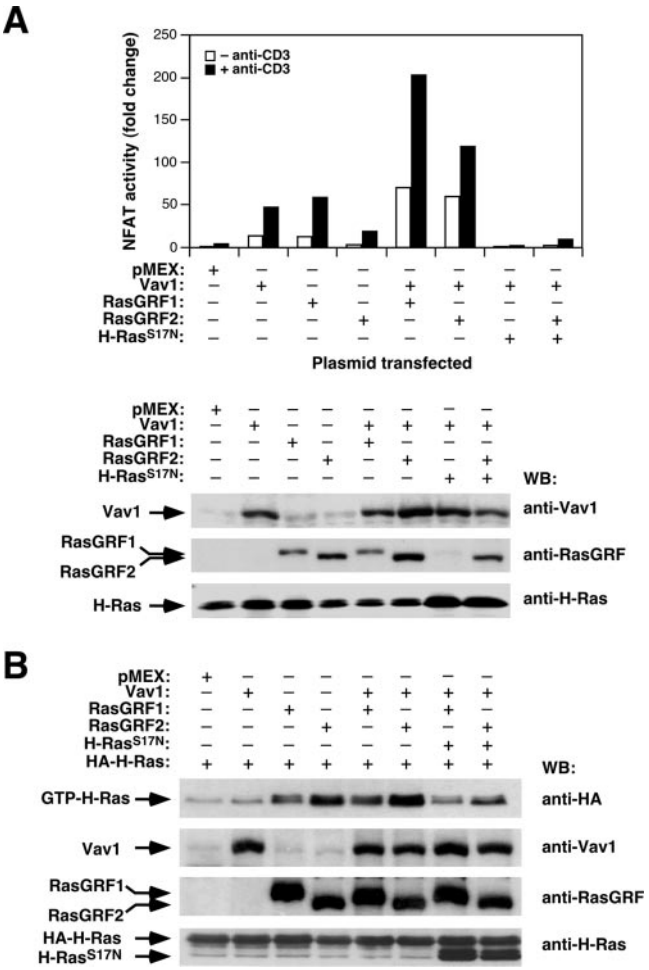

FIG. 4. RasGRF proteins synergize with Vav1 in a Ras-dependent manner for NF-AT activation. (A) Jurkat cells expressing the indicated proteins and the pNF-AT*luc* reporter plasmid were stimulated with anti-CD3 antibodies as indicated and subjected to NF-AT assays (upper panel). Aliquots of total cellular lysates were subjected to immunoblot analysis with the indicated antibodies (right) to monitor the level of expression of the proteins used in this experiment (lower panel). (B) Jurkat cells expressing HA-H-Ras, either alone or in combination with the indicated molecules, were subjected to GST-RBD pulldown experiments as indicated in the legend to Fig. 1. WB, Western blot.

totally incapable of activating H-Ras under the same conditions (Fig. 5B, protein 6). The rest of the RasGRF1 mutants used could promote more GTP loading of H-Ras with the wild-type RasGRF1 protein (Fig. 5B). The RasGRF2 mutant lacking the IQ region also induced normal levels of GDP/GTP exchange in the cotransfected H-Ras protein (Fig. 5B). However, when those mutants were tested in NF-AT assays, we observed that only the RasGRF1 PH1 domain was dispensable for the engagement of this signaling pathway (Fig. 5C). In contrast, mutations affecting the rest of the domains significantly reduced (in the case of the L263Q and PH2 mutants, see the scheme in Fig. 5A) or totally eliminated (the rest of mutants) the induction of NF-AT by RasGRF1 (Fig. 5C). Interestingly, the RasGRF1 mutant lacking the Ras GEF domain (ΔCdc25 protein; Fig. 5A) was inactive and, at the same time, appeared to act as a dominant-negative mutant since its expression totally blocked the low levels of NF-AT activity detected in the mock-transfected Jurkat cells (Fig. 5C, compare bars labeled as "pMEX" and "6"). In the case of RasGRF2, an analogous mutant was previously described as a dominant-negative mutant in nonhematopoietic cells (21). The elimination of the IQ domain in RasGRF2 also abrogated the stimulation of NF-AT by this protein in nonstimulated, anti-CD3-stimulated, and ionomycin-treated cells (Fig. 5D). Since all these RasGRF mutants can activate Ras (Fig. 5B), these results indicate that additional routes to the Ras pathway have to be assembled by RasGRF proteins in order to promote the stimulation of the transcriptional factor NF-AT. Similar results were obtained when the NF-AT activity was measured in cells coexpressing Vav1 with RasGRF1 mutants (Ruiz and Bustelo, unpublished). Under these conditions, the RasGRF1ΔCdc25 mutant protein also blocked the NF-AT stimulation induced by Vav1 (Ruiz and Bustelo, unpublished), suggesting that this RasGRF1 mutant protein works as a dominant-negative protein during T-cell signaling. However, the overexpression of a truncated, dominant-negative Vav1 protein containing only the SH3-SH2-SH3 region also promoted the inhibition of RasGRF2-dependent responses (Ruiz and Bustelo, unpublished), indicating that Vav1 and RasGRF2 work in independent parallel routes that are required for NF-AT activation or, alternatively, that they share a common signaling element that is sequestered by the overexpressed dominant-negative mutants. All together, these observations further suggest that RasGRF proteins, in addition to promoting the stimulation of the Ras/ERK pathway, probably contribute to NF-AT activation through the engagement of parallel signal transduction pathways.

Ca^{2+} and PLC-γ1 activity are both required for effective NF-AT stimulation by RasGRF and Vav1 proteins. To identify the pathways that in addition to Ras contribute to the activation of NF-AT by RasGRF proteins, we determined whether the RasGRF-mediated signals could depend on the generation of Ca^{2+} fluxes. To this end, we evaluated the effect of the pretreatment of Jurkat cells with BAPTA, a Ca^{2+}-specific chelator, in the Vav1- and RasGRF-dependent activation of NF-AT. This drug inhibited the stimulation of NF-AT in the mock-, Vav1-, and RasGRF2-transfected cells (Ruiz and Bustelo, unpublished), indicating that Ca^{2+} does play roles in the signaling pathway of those molecules. Since Ca^{2+} fluxing is initially triggered by inositol triphosphate, a second messenger generated by PLC-γ1 (18), we also tested the effect of overexpressing a PLC-γ1 dominant-negative protein (Y783F mutant) on the Vav1- and RasGRF-dependent stimulation of NF-AT. As shown in Fig. 6A, the PLC-γ1(Y783F) mutant protein, but not its wild-type counterpart, impaired both the basal and the anti-CD3-stimulated NF-AT activity induced by Vav1 and the two RasGRF proteins. In addition, it also inhibited the synergistic response observed upon the cotransfection of RasGRF family members with Vav1 (Fig. 6A). Consistent with these results, we observed that the stimulation of NF-AT by both Vav1 and RasGRF proteins did not occur in mutant Jurkat cell lines deficient for PLC-γ1 activity, such as those lacking expression of either the LAT adaptor or PLC-γ1 itself (Ruiz and Bustelo, unpublished). Taken together, these results indicate that the NF-AT activation in Vav1-, RasGRF1-, RasGRF2-,

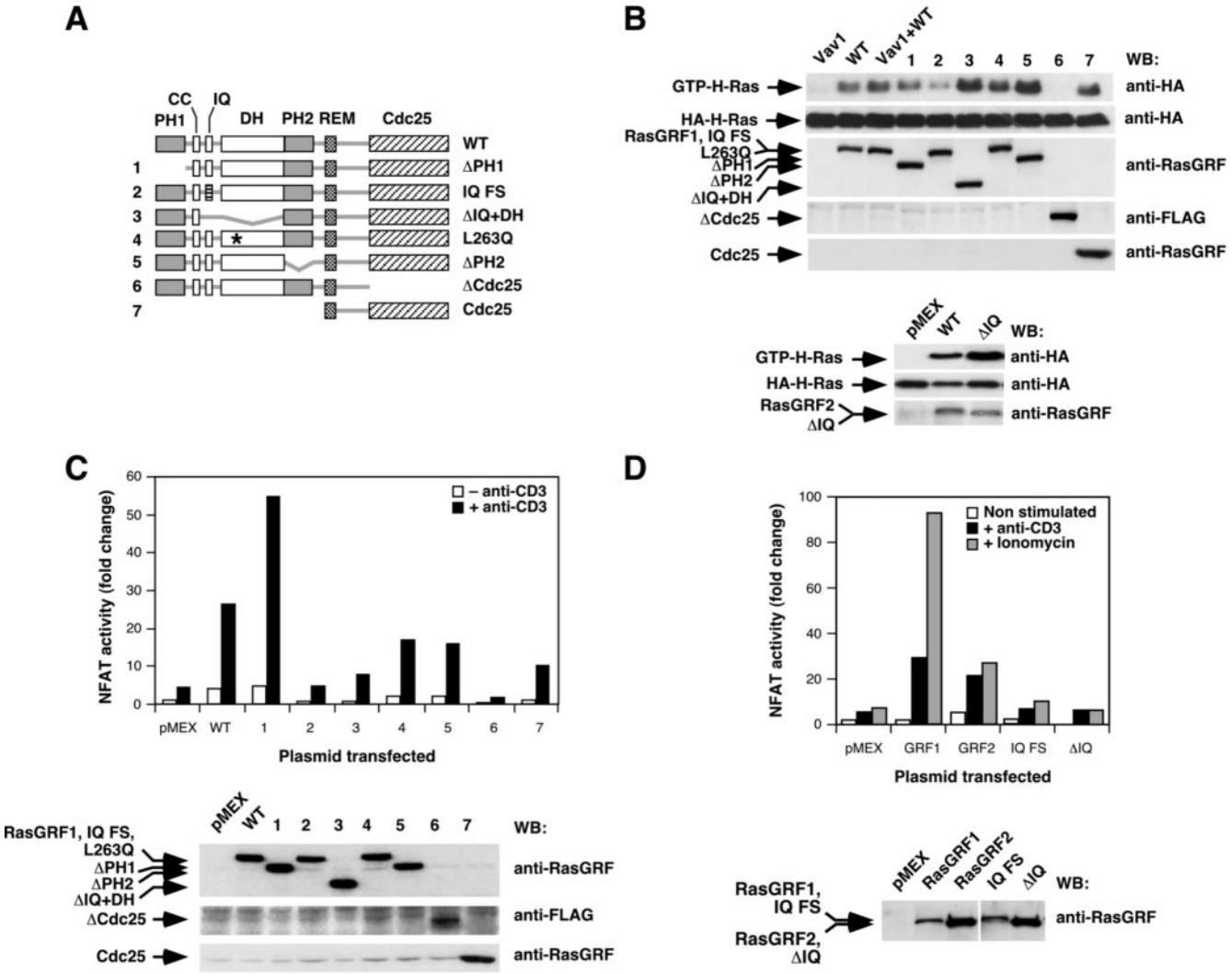

FIG. 5. Structural determinants involved in the activation of NF-AT by RasGRF proteins. (A) Schematic representation of the mutant RasGRF1 proteins used in these experiments. The RasGRF2 ΔIQ protein (not depicted here) lacked only the entire IQ region, as indicated in Materials and Methods. (B) Activation of HA-H-Ras by RasGRF1 (top panels) and RasGRF2 (bottom panels) mutants. Jurkat cells expressing the HA-H-Ras in the presence of the indicated proteins (top) were subjected to GST-RBD pulldown experiments as indicated in Materials and Methods. The expression of the proteins used in the experiment was assessed in aliquots from the same lysates by immunoblot analysis with the indicated antibodies (right). (C and D) Activation of NF-AT by RasGRF1 (C and D) and RasGRF2 (D) proteins determined in the stimulation conditions indicated (upper panels). Aliquots of the total cellular lysates were processed in parallel to determine the level of expression of the transfected proteins (C and D, lower panels). In the histogram of panel D, RasGRF1 and RasGRF2 have been abbreviated as GRF1 and GRF2, respectively. WT, wild type; WB, Western blot; CC, coiled-coil motif; FS, frameshift; *, point mutation.

and Vav1/RasGRF-expressing cells depends on both Ras and the generation of PLC-γ1-dependent Ca^{2+} fluxes.

Given the similarities observed between the behavior of Vav1 and RasGRF proteins in triggering the NF-AT response, we decided to investigate whether RasGRF proteins could influence, like Vav1 (11, 43, 61), the phosphorylation status of PLC-γ1. We observed that RasGRF2 and, to a lower extent, RasGRF1 could induce the phosphorylation of PLC-γ1 in nonstimulated cells (Fig. 6B). The levels of PLC-γ1 phosphorylation induced by RasGRF2 were similar to those obtained by overexpressing Vav1, although approximately two- to threefold lower than those induced by direct TCR stimulation (Fig. 6B). Reblotting of the filter with antibodies to the HA epitope confirmed the presence of equal levels of immunoprecipitated PLC-γ1 in all samples analyzed (Fig. 6B).

To verify whether these two proteins could interact physically in vivo, we next performed coimmunoprecipitation experiments with FLAG-tagged RasGRF2 and HA-tagged PLC-γ1. These assays were conducted in 293T cells because their high transfection efficiencies traditionally allow the detection of low stoichiometry interactions. As shown in Fig. 6C, we could detect PLC-γ1 in the anti-FLAG immunoprecipitates, but only when the FLAG-RasGRF2 protein was present in the 293T lysates. In the reverse coimmunoprecipitation protocol, we also detected RasGRF2 in HA-PLC-γ1 immunoprecipitates (Fig. 6C). In similar experiments, we also observed the recip-

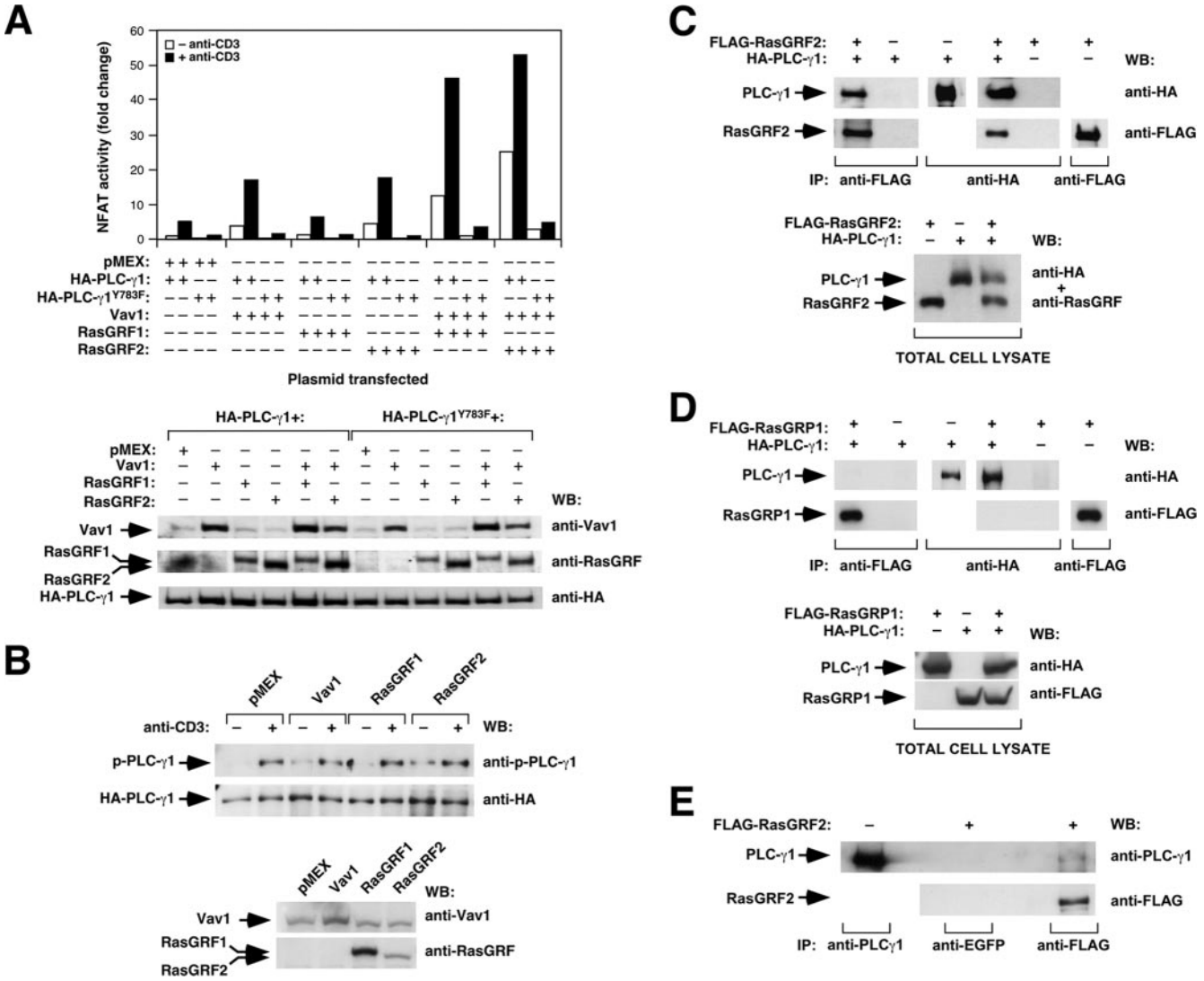

FIG. 6. Relationship of the RasGRF2 pathway with the PLC-γ1 route. (A) Activation levels of NF-AT in Jurkat cells expressing the indicated combinations of Vav1 and RasGRF proteins in the presence of either the wild-type or the dominant-negative (Y783F mutant) versions of PLC-γ1 (upper panel). The expression level of each protein under these conditions was determined in aliquots of the same cell lysates (bottom panels) using Western blot analysis with the indicated antibodies (right). (B) Total cellular lysates from nonstimulated (−) and anti-CD3-stimulated (+) Jurkat cells expressing the indicated proteins were immunoprecipitated with anti-HA antibodies. The phosphorylation levels of PLC-γ1 were then determined with an antibody to the phosphorylated Y783 residue of this phospholipase (top panel). Filters were then reblotted with anti-HA antibodies to reveal the amount of total PLC-γ1 immunoprecipitated under each condition (lower panel). (C and D) 293T cells not expressing (−) or expressing (+) FLAG-tagged RasGRF2 (C), FLAG-tagged RasGRP1 (D), and/or HA-tagged PLC-γ1 (C and D) proteins were subjected to coimmunoprecipitation experiments using either anti-HA or anti-FLAG antibodies (C and D). The presence of the immunoprecipitated and coimmunoprecipitated proteins was then determined by immunoblot analysis (C and D, upper panels). The appropriate expression of FLAG-RasGRF2 (C, bottom panel), FLAG-RasGRP1 (D, bottom panel), and HA-PLC-γ1 (C and D, bottom panels) was also confirmed using a Western blot with a pool of anti-HA plus anti-RasGRF antibodies (C) or two separate immunoblots with anti-HA and anti-FLAG antibodies (D). (E) Jurkat cells not expressing (−) or expressing (+) ectopic FLAG-tagged RasGRF2 were subjected to coimmunoprecipitation experiments using anti-FLAG antibodies and, as a negative control, anti-EGFP antibodies. As a positive control, the endogenous PLC-γ1 was immunoprecipitated with anti-PLC-γ1 antibodies (upper panel). Immunoprecipitates were then subjected to Western blot analysis with anti-PLC-γ1 antibodies (upper panel). After this step, the filter was stripped and reblotted with anti-FLAG antibodies (bottom panel). IP, immunoprecipitation; WB, Western blot.

rocal association of HA-PLC-γ1 and RasGRF1 (Ruiz and Bustelo, unpublished). In contrast, we could not detect any association between HA-PLC-γ1 and a FLAG-tagged version of RasGRP1 under identical experimental conditions (Fig. 6D), indicating that the coimmunoprecipitation of PLC-γ1 with RasGRF2 is a specific event. The significance of these results was further strengthened by the observation that FLAG-tagged RasGRF2 could associate with the endogenous PLC-γ1 when transfected in Jurkat cells (Fig. 6E). The poor sensitivity of the anti-RasGRF antibodies precluded the analysis of the interaction of the endogenous RasGRF2 and PLC-γ1 proteins (Ruiz and Bustelo, unpublished). Taken together, these results

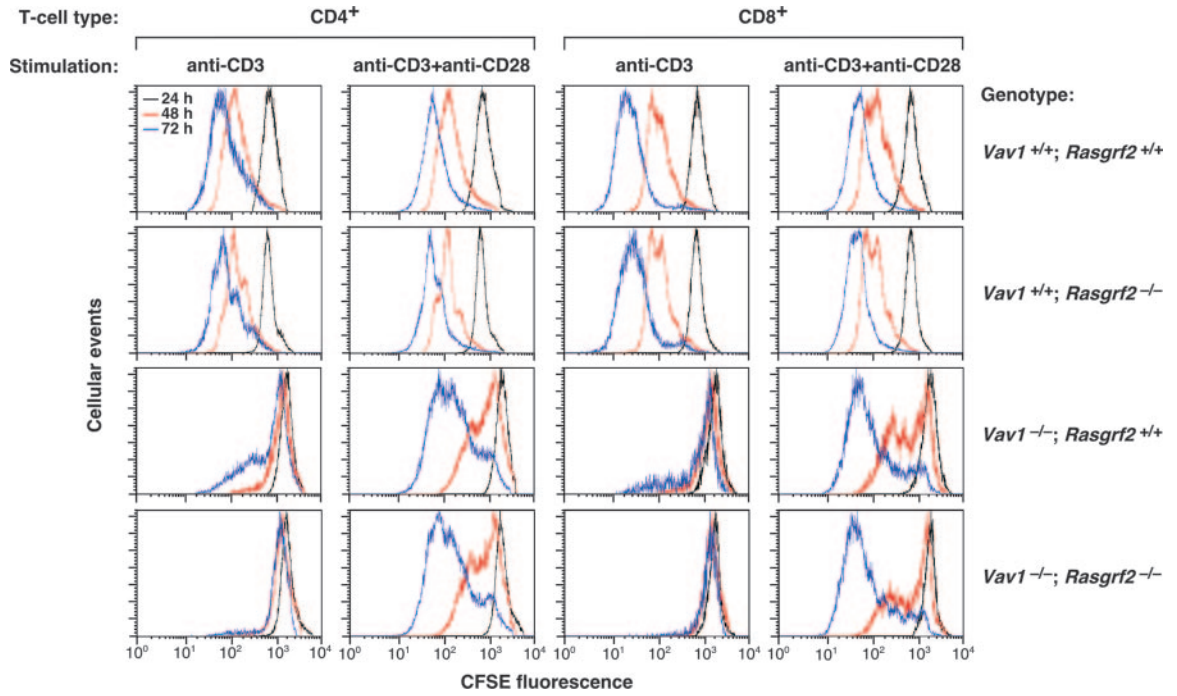

FIG. 7. Cell division rates of splenic T lymphocytes from wild-type, *Vav1*$^{-/-}$, *Rasgrf2*$^{-/-}$, and *Vav1*$^{-/-}$; *Rasgrf2*$^{-/-}$ mice. CSFE-loaded splenic cells derived from the indicated mice (right) were stimulated with anti-CD3 or anti-CD3 plus anti-CD28 antibodies (top). After the indicated periods of time, cells were collected and CSFE fluorescence measured in the CD4$^+$ and CD8$^+$ T-cell populations by flow cytometry. Representative graphs of a single experiment are shown. A minimum of 10,000 live cells was scored to generate each graph. The CSFE intensity profiles obtained at 24, 48, and 72 h poststimulation are shown in black, red, and blue, respectively. Similar results were obtained in four additional independent experiments (see Table 1).

indicate that RasGRF2 is directly connected to the PLC-γ1 pathway and that, at least in T cells, such a connection results in increased phosphorylation levels of this phospholipase.

RasGRF2 contributes to TCR-dependent responses of mature T cells. In order to evaluate the physiological relevance of those observations in vivo, we decided to investigate whether the inactivation of the *rasgrf2* locus could induce dysfunctions in the development and/or effector functions of T lymphocytes. Since we were concerned about the functional redundancy of the Vav1/RasGRP1- and RasGRF2-mediated routes, we decided to include in these experiments the *Vav1*$^{-/-}$ mice and a double-knockout animal containing null alleles for both *vav1* and *rasgrf2* genes. The analysis of these mice found no dysfunctions in the ontogeny of T cells, indicating that RasGRF2 is not essential for the pre-TCR selection checkpoint or the positive selection of TCR-bearing thymocytes (Ruiz and Bustelo, unpublished). To verify whether this GEF has roles in TCR-dependent responses of mature T cells, we next used carboxyfluorescein diacetate succinimidyl ester (CSFE)-labeling experiments to compare the cell division cycles of wild-type T lymphocytes with those of RasGRF2-, Vav1-, and RasGRF2/Vav1-deficient T cells. As expected (49, 58), splenic *Vav1*$^{-/-}$ T cells showed a serious proliferation deficit even after 72 h of stimulation with saturating concentrations of anti-CD3 antibodies and, to a lower extent, upon the simultaneous engagement of CD3 and CD28 receptors (Fig. 7; Table 1). *Rasgrf2*$^{-/-}$ T cells displayed no significant changes in their proliferation potential (Fig. 7; Table 1). However, we observed that the combined inactivation of *rasgrf2* and *vav1* genes further aggravated the defective proliferation rates induced by the single

TABLE 1. Proliferation of splenic T cells from mice of the indicated genotypes

Mouse genotype	% of undivided cells stimulated with indicated antibodies for the indicated times (h)[a]							
	CD4$^+$				CD8$^+$			
	Anti-CD3		Anti-CD3 + Anti-CD28		Anti-CD3		Anti-CD3 + Anti-CD28	
	48	72	48	72	48	72	48	72
Vav1$^{+/+}$; *Rasgrf2*$^{+/+}$	8.04 ± 3.30	4.33 ± 1.01	1.73 ± 0.42	1.12 ± 0.20	10.10 ± 1.44	2.97 ± 1.57	2.63 ± 0.05	0.46 ± 0.06
Vav1$^{+/+}$; *Rasgrf2*$^{-/-}$	8.41 ± 1.35	4.35 ± 1.52	4.49 ± 0.98	2.42 ± 0.46	7.27 ± 1.60	3.70 ± 0.14	2.38 ± 1.57	1.33 ± 0.48
Vav1$^{-/-}$; *Rasgrf2*$^{+/+}$	75.45 ± 5.26	63.15 ± 6.42	44.13 ± 1.4	17.98 ± 3.87	80.82 ± 2.14	68.98 ± 3.89	37.34 ± 0.02	9.92 ± 2.62
Vav1$^{-/-}$; *Rasgrf2*$^{-/-}$	95.42 ± 2.37	88.73 ± 7.03	48.36 ± 5.36	20.25 ± 4.87	92.77 ± 1.89	89.98 ± 8.47	54.03 ± 6.60	15.84 ± 3.92

[a] Percentages shown are from five experiments. See Materials and Methods for further technical details.

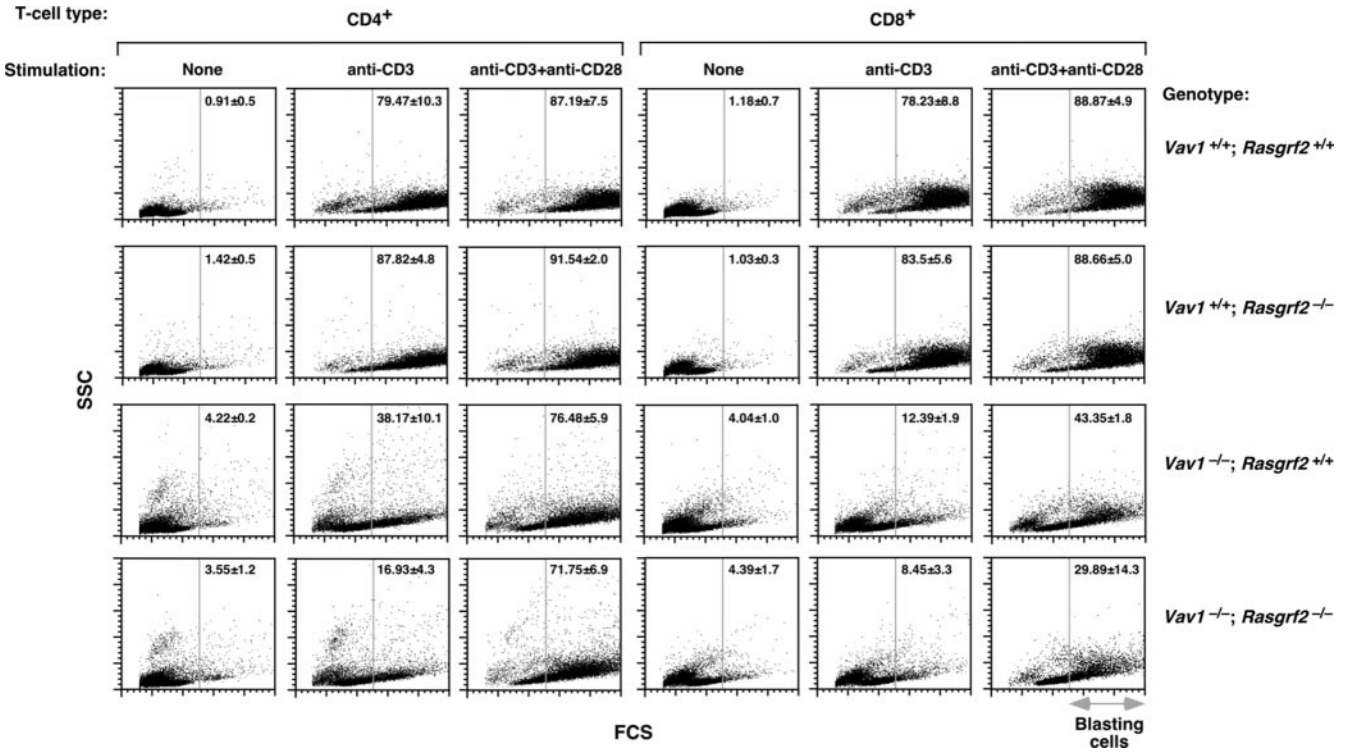

FIG. 8. Blast formation in wild-type, *Vav1*$^{-/-}$, *Rasgrf2*$^{-/-}$, and *Vav1*$^{-/-}$; *Rasgrf2*$^{-/-}$ mice. Splenic cells derived from the indicated knockout mice (right) were stimulated as shown (top). After 24 h, cells were collected and blasts formed in the CD4$^+$ and CD8$^+$ T-cell populations were analyzed by flow cytometry. Forward-scatter dot blots in CD4$^+$- and CD8$^+$-gated cells in a representative experiment are shown ($n = 5$). In the *y* and *x* axes, the SSC and FCS values range from 0 to 1,024, respectively. Numbers represent the means and standard deviations of the percentages (%) of blasting cells in the indicated experimental conditions analyzed. The vertical gray lines indicate the FCS point from where gated cells have been considered as blasts. Note that the reduction in the blasting population in anti-CD3/anti-CD28-stimulated *Vav1*$^{-/-}$; *Rasgrf2*$^{-/-}$ CD8$^+$ cells (right bottom panel) is not statistically significant. SSC, side scatter; FCS, forward scatter.

vav1 inactivation in anti-CD3-stimulated CD4$^+$ and CD8$^+$ T cells. In the case of helper T cells, this proliferative blockage could be restored to the levels observed in *Vav1*$^{-/-}$ deficient T cells upon stimulation with anti-CD3 plus anti-CD28 antibodies (Fig. 7; Table 1). In the case of the *Vav1*$^{-/-}$; *Rasgrf2*$^{-/-}$ cytotoxic T cells, such restoration was only partial (Fig. 7; Table 1).

As an alternative method to measure T-cell proliferation, we examined the production of large (blasting) cells in cultures of stimulated splenocytes. Wild-type and *Rasgrf2*$^{-/-}$ CD4$^+$ T cells underwent normal levels of blast formation upon both anti-CD3 and anti-CD3 plus anti-CD28 treatment (Fig. 8). *Vav1*$^{-/-}$ CD4$^+$ T cells showed a reduction in the blast population (≈41.3 and 10.7% in anti-CD3- and anti-CD3/anti-CD28-stimulated cells, respectively; Fig. 8). This defect was further accentuated (≈62.5%) in anti-CD3-stimulated *Vav1*$^{-/-}$; *Rasgrf2*$^{-/-}$ CD4$^+$ lymphocytes (Fig. 8). The costimulation with anti-CD28 antibodies rescued that defect, increasing the blast percentage of *Vav1*$^{-/-}$; *Rasgrf2*$^{-/-}$ cells to levels similar to those found in *Vav1*$^{-/-}$ T cells (Fig. 8). Similar results were observed in CD8$^+$ T cells (Fig. 8).

To correlate the above defects with intracellular responses, we then examined by flow cytometry the expression of molecules that are induced in T cells through the Ras pathway alone (CD69) (19), the calcineurin route alone (TNF-α) (33), or the simultaneous triggering of Ras and calcineurin pathways (IL-2) (55). The single *rasgrf2* gene deficiency affected only marginally the surface marker CD69 induced upon TCR cross-linking (Fig. 9A). No statistically significant defects in the expression of this marker were observed in *Rasgrf2*$^{-/-}$ CD4$^+$ T cells when stimulated with anti-CD3 plus anti-CD28 antibodies (Fig. 9A). Similar results were obtained even when T cells were stimulated with suboptimal concentrations of anti-CD3 antibodies (Ruiz and Bustelo, unpublished), indicating that the RasGRF2 deficiency does not affect significantly the Ras pathway. In agreement with these results, we could not observe any significant defects in the activation of ERKs in either TCR-stimulated splenic or thymic T cells derived from *Rasgrf2*$^{-/-}$ mice (Fig. 9B). However, and as expected (16, 31), the Vav1 deficiency did induce a severe defect in ERK activation in these two cell populations (Fig. 9B). In contrast to the above results, we observed that *Rasgrf2*$^{-/-}$ cells did show an ≈50% reduction in the expression levels of both IL-2 and TNF-α upon stimulation with anti-CD3 either alone (in the case of TNF-α) or in combination with anti-CD28 antibodies (in the case of both IL-2 and TNF-α) (Fig. 9A). This lower efficiency in IL-2 synthesis does not appear to be dramatic from a functional point of view, because *Rasgrf2*$^{-/-}$ T cells show normal proliferation rates in culture (see above) (Fig. 7). The impairment in IL-2 and TNF-α production in *Rasgrf2*$^{-/-}$ cells was nevertheless smaller that that observed in Vav1-deficient CD4$^+$ T cells (Fig.

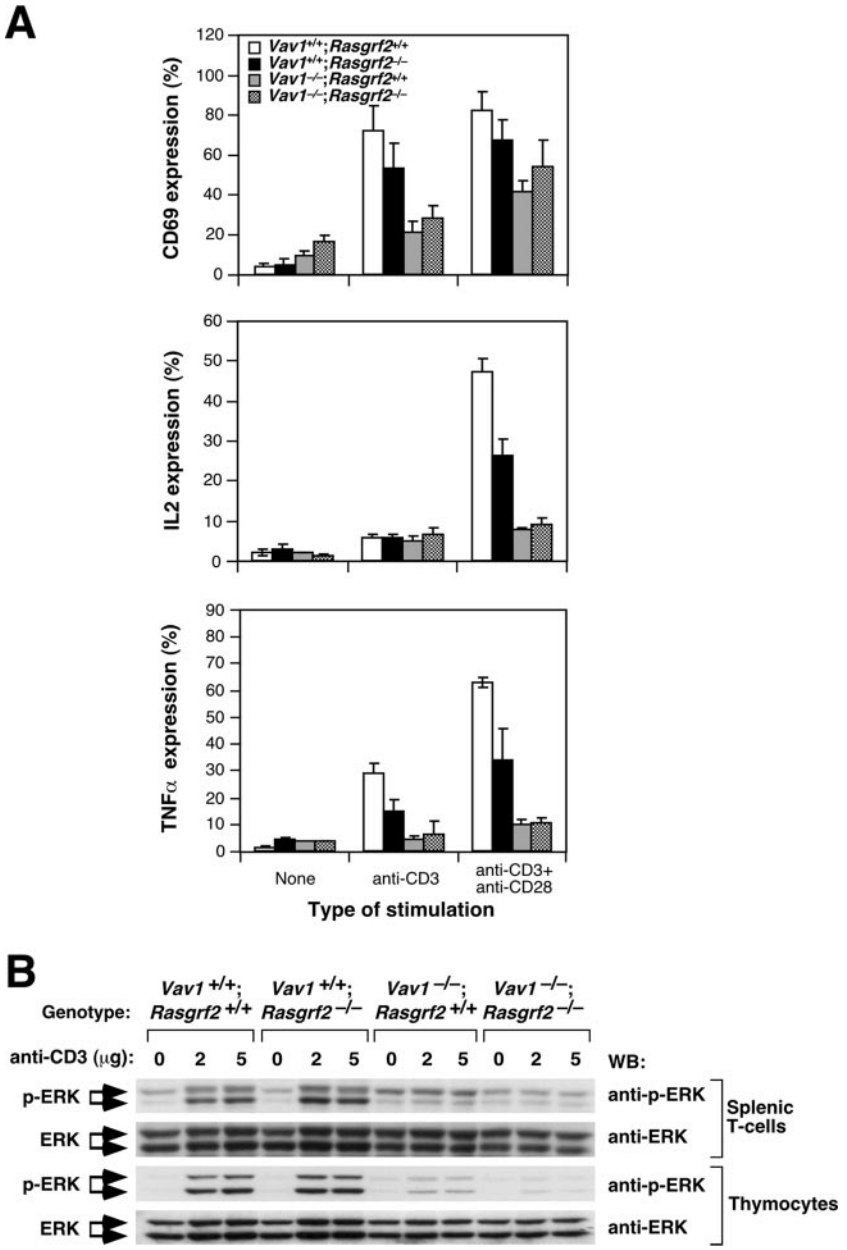

FIG. 9. Effect of the inactivation of *rasgrf2* gene on short-term and long-term signaling responses. (A) Splenic cells obtained from animals of the indicated genotypes were stimulated with either anti-CD3 or anti-CD3 plus anti-CD28 antibodies for 6 h. After this period, cells were collected, stained with anti-CD4 antibodies, and monitored by flow cytometry to quantify the percentages of $CD4^+$ T cells positive for CD69 (top panel), IL-2 (middle panel), and TNF-α (bottom panel). A minimum of 10,000 live cells was scored in each condition. Graphs represent the means and standard deviations obtained in five independent experiments. (B) Splenic and thymic T cells were obtained from mice of the indicated genotypes (top), incubated with the indicated amounts of anti-CD3 antibodies (top), and cross-linked with secondary antibodies as indicated in Materials and Methods. After 3 min, cells were lysed and clarified extracts subjected to immunoblot analysis using antibodies to either phosphorylated (first and third panels from top) or total ERK (second and fourth panels from top). WB, Western blot.

9A), which do experience lower proliferation levels (see above) (Fig. 7). The *Vav1*$^{-/-}$; *Rasgrf2*$^{-/-}$ double mutation did not worsen the already strong defect in CD69, IL-2, and TNF-α production observed upon the single deletion of the *vav1* proto-oncogene (Fig. 9A). Combined with the proliferative assays, these results confirm that RasGRF2 plays an important, although ancillary, role in the main Vav1/RasGRP1 route during TCR-dependent responses.

DISCUSSION

The crucial role played by the Ras pathway in the life of T cells has fueled the interest in the identification of the GDP/GTP exchange factors involved in the activation of Ras family GTPases in both immature and differentiated T cells. These studies have revealed that RasGRP1 and, to a lower extent, Sos proteins play specific roles in this functional context (23,

45). In this report, we show that RasGRF2, a Ras regulator belonging to an independent GEF family (42), also participates in the T-cell signaling machinery. Consistent with this role, we have shown that this protein is expressed in both immature and mature T cells and that, when overexpressed in Jurkat cells, it translocates to the immune synapse, induces Ras activation, and promotes the stimulation of NF-AT activity. While the levels of Ras activation induced by RasGRF2 remain constant independently of the type of stimulation induced in the Jurkat cell, RasGRF2 does synergize with the TCR, Ca^{2+}, and Vav1 pathways in order to induce robust NF-AT activation levels. To confirm that the implication of RasGRF2 in TCR signaling also occurred in vivo, we analyzed the influence of RasGRF2 in the development and signaling of T cells using *Rasgrf2*$^{-/-}$ mice. To bypass the problem of the prevalent role of RasGRP1 in T-cell signaling events (23), we decided to combine the use of *Rasgrf2*$^{-/-}$ mice with animals lacking expression of both RasGRF2 and RasGRP1. Given that *Rasgrp1*$^{-/-}$ animals produce highly reduced numbers of peripheral T cells that preclude the analysis of the T-cell compartment in *Rasgrf2*$^{-/-}$; *Rasgrp1*$^{-/-}$ mice (23), we decided to use an alternative double-knockout mouse strain containing null alleles for both the *vav1* and *rasgrf2* genes. *Vav1*$^{-/-}$ animals can be considered as having a hypomorphic mutation of RasGRP1 because, due to the residual presence of Vav2 and Vav3 in T lymphocytes, they display low but significant levels of RasGRP1 activation upon pre-TCR and TCR engagement (31). Therefore, these animals allow the study of the contribution of RasGRF2 under suboptimal conditions of RasGRP1 activity. These analyses indicated that RasGRF2 per se does not have any major role in IL-7-receptor-dependent stages of thymocyte development, in the β checkpoint, in positive selection, or in lineage commitment (data not shown). In the case of mature T cells, we observed that the absence of this RasGEF affects predominantly the expression NF-AT-dependent cytokines such as IL-2 and TNF-α. This defect was however significantly milder than that found in *Vav1*$^{-/-}$ cells and, in fact, it did not induce any detectable defects in the blasting and proliferation of *Rasgrf2*$^{-/-}$ cells. Interestingly, the lack of RasGRF2 induced no major changes in either proximal elements of the Ras pathway (i.e., ERK activation) or direct Ras-dependent biological responses such as the expression of the CD69 marker, suggesting that the impaired NF-AT responses found in these cells are not probably due to inefficient output signal from the PLC-γ1/calcineurin branch rather than from diminished activation of the Ras pathway. While the concurrent inactivation of the *rasgrf2* and *vav1* loci did not aggravate the defects observed in the β checkpoint and positive selection of *Vav1*$^{-/-}$ cells, we observed that the RasGRF2 deficiency accentuated both the blasting and proliferative defects found in anti-CD3-stimulated $CD4^+$ and $CD8^+$ splenic T lymphocytes. This defect was rescued totally or partially when $CD4^+$ and $CD8^+$ cells were costimulated with the CD28 receptor, respectively. Taken together, these results indicate that RasGRF2 plays an important, although ancillary, role in the RasGRP1 route during the TCR-dependent responses of mature T cells.

What is the function of RasGRF2 in this cellular setting? In addition to promoting Ras activation in mature T lymphocytes, our signaling experiments suggest that RasGRF2 is primarily involved in Vav1-like functions such as the activation of the calcineurin phosphatase. Thus, we have shown that RasGRF2, like Vav1 (61), can promote tyrosine phosphorylation of PLC-γ1, an enzyme critical for both the DAG/RasGRP1-dependent stimulation of Ras and the Ca^{2+}/calmodulin-dependent activation of calcineurin (18). Consistent with this view, we have observed that RasGRF2 mimics the function of Vav1 in this response. For example, both RasGRF2 and Vav1 synergize with TCR- and Ca^{2+}-dependent signals to generate maximal NF-AT activation levels. Likewise, the NF-AT activity induced by Vav1 and RasGRF2 in nonstimulated Jurkat cells is inhibited by a dominant-negative mutant version of PLC-γ1. The basal NF-AT activities of Vav1 and RasGRF2 also show similar dependencies on LAT and PLC-γ1, as inferred from NF-AT assays conducted in Jurkat cell clones deficient for those proteins (Ruiz and Bustelo, unpublished). Our observations indicating that the NF-AT-dependent responses (*il2* and *tnfα* gene expression) are more affected than the Ras-dependent pathways (i.e., *cd69* gene expression) in *Rasgrf2*$^{-/-}$ T cells suggest that, in fact, the induction of properly balanced levels of NF-AT activation is probably the main role of this GEF in stimulated T cells.

The mechanism by which RasGRF2 promotes PLC-γ1 and NF-AT activation remains unknown. This protein shares some structural domains with Vav1, such as the DH-PH cassette involved in Rac1 activation in both proteins (17, 26). However, this structural similarity cannot solely explain the common effector functions, because we and others have shown that other highly related GEFs such as Vav2, Sos1, and RasGRP1 do not promote NF-AT activity in the same cellular and signaling settings (this work; see also references 5 and 22). Given that NF-AT activation requires the involvement of multiple structural domains of RasGRF proteins (this work) and Vav1 (62), it is anticipated that RasGRF action in this route will probably entail the assembly of multiple signal transduction molecules and/or regulatory events that cooperate in the generation of optimal NF-AT-mediated signaling outputs by T cells. In any case, it is likely that the Vav1 and RasGRF2 pathways overlap in that response, given our observation that the dominant-negative mutants of these two proteins inhibit the activation of NF-AT triggered by the activation of both Vav1 and RasGRF2. Moreover, the activation of NF-AT and Ras by RasGRF proteins probably represents two intertwined but mechanistically independent steps, because we have identified RasGRF mutants that, despite their ability to promote normal levels of Ras activation, cannot trigger proper NF-AT responses. Further work in this area with Vav1 and RasGRF2 will be needed to identify the signaling elements that mediate this important intracellular pathway.

Taken together, these results are consistent with a new model for the activation of NF-AT in T cells that integrates the participation of the exchange factors Vav1, RasGRP1, Sos1, and RasGRF2 (Fig. 10). In this model, Vav1 and RasGRP1 define the prevalent pathway involved in both Ras and NF-AT activation, whereas RasGRF2 and Sos1 play subsidiary roles. This model presents multiple sites of positive feedbacks emanating from PLC-γ1 that could contribute to the amplification of the downstream NF-AT signal. Thus, the DAG generated by the Vav1- and RasGRF2-mediated activation of PLC-γ1 can favor Ras activation via the direct activation of RasGRP1 by DAG and, indirectly, through the phosphorylation of that ex-

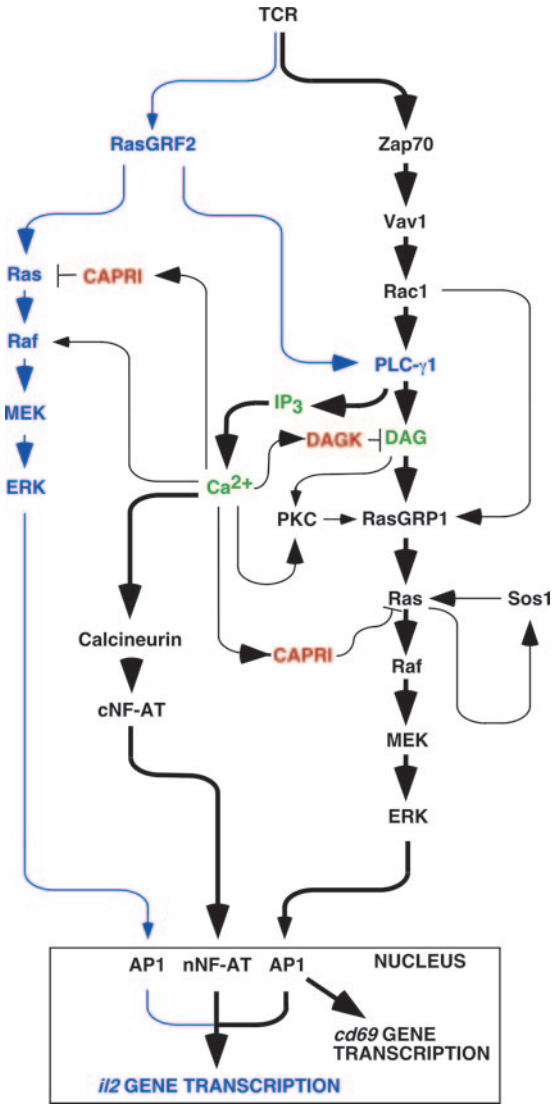

FIG. 10. A schematic view of Ras- and calcineurin-dependent pathways in T cells. The known components of the combined pathway are shown in black. The new pathway described in this work is shown in blue. The main second messengers are indicated in green. Negative regulators of T-cell signaling operating in this pathway are shown in red. Thicker arrows highlight the prevalence of the Vav1/RasGRP1 pathway over the rest of signaling connections presented in this figure. For the sake of simplicity, we have not included adaptor proteins and kinases involved in the pathway. Likewise, we have omitted other transcriptional factors that cooperate in the transcription of NF-AT-regulated genes. The direct connection between Rac1 and RasGRP1 is based on previous observations indicating that the polymerization of F-actin by Rac1 contributes to the translocation of RasGRP family members to the plasma membrane (11, 12). Other regulatory points are discussed in the main text.

change factor by PKC (43, 44, 61). In addition, it has been previously shown that Ca^{2+} synergizes with the RasGRF-mediated activation of Ras to promote optimal levels of ERK stimulation in nonhematopoietic cells (2, 21). This synergistic action appears to be established at the level of c-Raf1 (2). It is also possible that Ca^{2+} could also affect directly RasGRP1 and RasGRF2 because both proteins contain Ca^{2+}-binding domains (42). However, the action of Ca^{2+} on these GEFs is probably not exerted from an upstream position, as evidenced by the lack of activation of Ras GTPases in calcium ionophore-treated T cells. The multiple, positive effects of Ca^{2+} on the Ras pathway probably bypass, in the early stimulation times, its subsequent inhibitory actions on the same route that are exerted through CAPRI, a Ca^{2+}-regulated RasGAP, and the α isoform of DAG-kinase, a Ca^{2+}-dependent enzyme that hydrolyzes DAG to yield phosphatidic acid (18). Despite the fact that RasGRF1 is not expressed in lymphocytes, we have observed that it induces reproducibly stronger signals in T cells than RasGRF2. It will be interesting to verify therefore whether some of the signaling connections reported here could be extrapolated to other cell systems where RasGRF1 plays essential roles (i.e., neurons and pancreatic β cells).

ACKNOWLEDGMENTS

X.R.B.'s work is supported by grants from the U.S. National Cancer Institute/NIH (5R01-CA73735-10), the Spanish Ministry of Education and Science (MES) (SAF2006-01789), the Castilla-León Autonomous Government (SA053A05), and the Red Temática de Investigación Cooperativa en Cáncer (RTICC) (RD06/0020/0001), Fondo de Investigaciones Sanitarias (FIS), Carlos III Institute, Spanish Ministry of Health. E.S. is supported by grants from the MES (GEN2003-20239-C062) and FIS (PI061274, RD06/0020/0000). S.R. has been partially supported by the NCI/NIH and the MES Juan de la Cierva program. All Spanish funding is cosponsored by the European Union FEDER program.

We thank B. Alarcón and P. Delgado for their initial help for setting up the immune synapse experiments, J. Almeida and A. Orfao for help in the T-cell stimulation and flow cytometry experiments, V. Tybulewicz for his generous gift of *vav1*$^{-/-}$ mice, J. Tamame and M. T. Blázquez for technical assistance, and M. J. Caloca for comments on the manuscript.

We declare no conflicts of interest related to this work.

REFERENCES

1. **Alberola-Ila, J., and G. Hernandez-Hoyos.** 2003. The Ras/MAPK cascade and the control of positive selection. Immunol. Rev. **191:**79–96.
2. **Anborgh, P. H., X. Qian, A. G. Papageorge, W. C. Vass, J. E. DeClue, and D. R. Lowy.** 1999. Ras-specific exchange factor GRF: oligomerization through its Dbl homology domain and calcium-dependent activation of Raf. Mol. Cell. Biol. **19:**4611–4622.
3. **Arozarena, I., D. Matallanas, M. T. Berciano, V. Sanz-Moreno, F. Calvo, M. T. Munoz, G. Egea, M. Lafarga, and P. Crespo.** 2004. Activation of H-Ras in the endoplasmic reticulum by the RasGRF family guanine nucleotide exchange factors. Mol. Cell. Biol. **24:**1516–1530.
4. **Augsten, M., R. Pusch, C. Biskup, K. Rennert, U. Wittig, K. Beyer, A. Blume, R. Wetzker, K. Friedrich, and I. Rubio.** 2006. Live-cell imaging of endogenous Ras-GTP illustrates predominant Ras activation at the plasma membrane. EMBO Rep. **7:**46–51.
5. **Billadeau, D. D., S. M. Mackie, R. A. Schoon, and P. J. Leibson.** 2000. The Rho family guanine nucleotide exchange factor Vav-2 regulates the development of cell-mediated cytotoxicity. J. Exp. Med. **192:**381–392.
6. **Bivona, T. G., I. Perez De Castro, I. M. Ahearn, T. M. Grana, V. K. Chiu, P. J. Lockyer, P. J. Cullen, A. Pellicer, A. D. Cox, and M. R. Philips.** 2003. Phospholipase Cgamma activates Ras on the Golgi apparatus by means of RasGRP1. Nature **424:**694–698.
7. **Bivona, T. G., and M. R. Philips.** 2003. Ras pathway signaling on endomembranes. Curr. Opin. Cell Biol. **15:**136–142.
8. **Brambilla, R., N. Gnesutta, L. Minichiello, G. White, A. J. Roylance, C. E. Herron, M. Ramsey, D. P. Wolfer, V. Cestari, C. Rossi-Arnaud, S. G. Grant, P. F. Chapman, H. P. Lipp, E. Sturani, and R. Klein.** 1997. A role for the Ras signalling pathway in synaptic transmission and long-term memory. Nature **390:**281–286.
9. **Bustelo, X. R., K. L. Suen, K. Leftheris, C. A. Meyers, and M. Barbacid.** 1994. Vav cooperates with Ras to transform rodent fibroblasts but is not a Ras GDP/GTP exchange factor. Oncogene **9:**2405–2413.
10. **Caloca, M. J., J. L. Zugaza, and X. R. Bustelo.** 2003. Exchange factors of the RasGRP family mediate Ras activation in the Golgi. J. Biol. Chem. **278:**33465–33473.
11. **Caloca, M. J., J. L. Zugaza, D. Matallanas, P. Crespo, and X. R. Bustelo.**

2003. Vav mediates Ras stimulation by direct activation of the GDP/GTP exchange factor Ras GRP1. EMBO J. **22:**3326–3336.
12. **Caloca, M. J., J. L. Zugaza, M. Vicente-Manzanares, F. Sanchez-Madrid, and X. R. Bustelo.** 2004. F-actin-dependent translocation of the Rap1 GDP/GTP exchange factor RasGRP2. J. Biol. Chem. **279:**20435–20446.
13. **Cen, H., A. G. Papageorge, W. C. Vass, K. E. Zhang, and D. R. Lowy.** 1993. Regulated and constitutive activity by CDC25Mm (GRF), a Ras-specific exchange factor. Mol. Cell. Biol. **13:**7718–7724.
14. **Chiu, V. K., T. Bivona, A. Hach, J. B. Sajous, J. Silletti, H. Wiener, R. L. Johnson II, A. D. Cox, and M. R. Philips.** 2002. Ras signalling on the endoplasmic reticulum and the Golgi. Nat. Cell Biol. **4:**343–350.
15. **Colicelli, J.** 2004. Human RAS superfamily proteins and related GTPases. Sci. STKE **2004:**RE13.
16. **Costello, P. S., A. E. Walters, P. J. Mee, M. Turner, L. F. Reynolds, A. Prisco, N. Sarner, R. Zamoyska, and V. L. Tybulewicz.** 1999. The Rho-family GTP exchange factor Vav is a critical transducer of T cell receptor signals to the calcium, ERK, and NF-kappaB pathways. Proc. Natl. Acad. Sci. USA **96:**3035–3040.
17. **Crespo, P., K. E. Schuebel, A. A. Ostrom, J. S. Gutkind, and X. R. Bustelo.** 1997. Phosphotyrosine-dependent activation of Rac-1 GDP/GTP exchange by the vav proto-oncogene product. Nature **385:**169–172.
18. **Cullen, P. J., and P. J. Lockyer.** 2002. Integration of calcium and Ras signalling. Nat. Rev. Mol. Cell Biol. **3:**339–348.
19. **D'Ambrosio, D., D. A. Cantrell, L. Frati, A. Santoni, and R. Testi.** 1994. Involvement of p21ras activation in T cell CD69 expression. Eur. J. Immunol. **24:**616–620.
20. **Daniels, M. A., E. Teixeiro, J. Gill, B. Hausmann, D. Roubaty, K. Holmberg, G. Werlen, G. A. Hollander, N. R. Gascoigne, and E. Palmer.** 2006. Thymic selection threshold defined by compartmentalization of Ras/MAPK signalling. Nature **444:**724–729.
21. **de Hoog, C. L., W. T. Fan, M. D. Goldstein, M. F. Moran, and C. A. Koch.** 2000. Calmodulin-independent coordination of Ras and extracellular signal-regulated kinase activation by Ras-GRF2. Mol. Cell. Biol. **20:**2727–2733.
22. **Doody, G. M., D. D. Billadeau, E. Clayton, A. Hutchings, R. Berland, S. McAdam, P. J. Leibson, and M. Turner.** 2000. Vav-2 controls NFAT-dependent transcription in B- but not T-lymphocytes. EMBO J. **19:**6173–6184.
23. **Dower, N. A., S. L. Stang, D. A. Bottorff, J. O. Ebinu, P. Dickie, H. L. Ostergaard, and J. C. Stone.** 2000. RasGRP is essential for mouse thymocyte differentiation and TCR signaling. Nat. Immunol. **1:**317–321.
24. **Ebinu, J. O., D. A. Bottorff, E. Y. Chan, S. L. Stang, R. J. Dunn, and J. C. Stone.** 1998. RasGRP, a Ras guanyl nucleotide-releasing protein with calcium- and diacylglycerol-binding motifs. Science **280:**1082–1086.
25. **Fam, N. P., W. T. Fan, Z. Wang, L. J. Zhang, H. Chen, and M. F. Moran.** 1997. Cloning and characterization of Ras-GRF2, a novel guanine nucleotide exchange factor for Ras. Mol. Cell. Biol. **17:**1396–1406.
26. **Fan, W. T., C. A. Koch, C. L. de Hoog, N. P. Fam, and M. F. Moran.** 1998. The exchange factor Ras-GRF2 activates Ras-dependent and Rac-dependent mitogen-activated protein kinase pathways. Curr. Biol. **8:**935–938.
27. **Fernandez-Medarde, A., L. M. Esteban, A. Nunez, A. Porteros, L. Tessarollo, and E. Santos.** 2002. Targeted disruption of Ras-Grf2 shows its dispensability for mouse growth and development. Mol. Cell. Biol. **22:**2498–2504.
28. **Fields, P. E., T. F. Gajewski, and F. W. Fitch.** 1996. Blocked Ras activation in anergic CD4+ T cells. Science **271:**1276–1278.
29. **Fischer, A. M., C. D. Katayama, G. Pages, J. Pouyssegur, and S. M. Hedrick.** 2005. The role of erk1 and erk2 in multiple stages of T cell development. Immunity **23:**431–443.
30. **Font de Mora, J., L. M. Esteban, D. J. Burks, A. Nunez, C. Garces, M. J. Garcia-Barrado, M. C. Iglesias-Osma, J. Moratinos, J. M. Ward, and E. Santos.** 2003. Ras-GRF1 signaling is required for normal beta-cell development and glucose homeostasis. EMBO J. **22:**3039–3049.
31. **Fujikawa, K., A. V. Miletic, F. W. Alt, R. Faccio, T. Brown, J. Hoog, J. Fredericks, S. Nishi, S. Mildiner, S. L. Moores, J. Brugge, F. S. Rosen, and W. Swat.** 2003. Vav1/2/3-null mice define an essential role for Vav family proteins in lymphocyte development and activation but a differential requirement in MAPK signaling in T and B cells. J. Exp. Med. **198:**1595–1608.
32. **Genot, E., and D. A. Cantrell.** 2000. Ras regulation and function in lymphocytes. Curr. Opin. Immunol. **12:**289–294.
33. **Goldfeld, A. E., E. Tsai, R. Kincaid, P. J. Belshaw, S. L. Schrieber, J. L. Strominger, and A. Rao.** 1994. Calcineurin mediates human tumor necrosis factor alpha gene induction in stimulated T and B cells. J. Exp. Med. **180:**763–768.
34. **Irvin, B. J., B. L. Williams, A. E. Nilson, H. O. Maynor, and R. T. Abraham.** 2000. Pleiotropic contributions of phospholipase C-γ1 (PLC-γ1) to T-cell antigen receptor-mediated signaling: reconstitution studies of a PLC-γ1-deficient Jurkat T-cell line. Mol. Cell. Biol. **20:**9149–9161.
35. **Kane, L. P., J. Lin, and A. Weiss.** 2000. Signal transduction by the TCR for antigen. Curr. Opin. Immunol. **12:**242–249.
36. **Li, S., X. Tian, D. M. Hartley, and L. A. Feig.** 2006. Distinct roles for Ras-guanine nucleotide-releasing factor 1 (Ras-GRF1) and Ras-GRF2 in the induction of long-term potentiation and long-term depression. J. Neurosci. **26:**1721–1729.
37. **Lopez-Lago, M., H. Lee, C. Cruz, N. Movilla, and X. R. Bustelo.** 2000. Tyrosine phosphorylation mediates both activation and downmodulation of the biological activity of Vav. Mol. Cell. Biol. **20:**1678–1691.
38. **Macian, F.** 2005. NFAT proteins: key regulators of T-cell development and function. Nat. Rev. Immunol. **5:**472–484.
39. **Martegani, E., M. Vanoni, R. Zippel, P. Coccetti, R. Brambilla, C. Ferrari, E. Sturani, and L. Alberghina.** 1992. Cloning by functional complementation of a mouse cDNA encoding a homologue of CDC25, a Saccharomyces cerevisiae RAS activator. EMBO J. **11:**2151–2157.
40. **Mor, A., G. Campi, G. Du, Y. Zheng, D. A. Foster, M. L. Dustin, and M. R. Philips.** 2007. The lymphocyte function-associated antigen-1 receptor costimulates plasma membrane Ras via phospholipase D2. Nat. Cell Biol. **9:**713–719.
41. **Perez de Castro, I., T. G. Bivona, M. R. Philips, and A. Pellicer.** 2004. Ras activation in Jurkat T cells following low-grade stimulation of the T-cell receptor is specific to N-Ras and occurs only on the Golgi apparatus. Mol. Cell. Biol. **24:**3485–3496.
42. **Quilliam, L. A., J. F. Rebhun, and A. F. Castro.** 2002. A growing family of guanine nucleotide exchange factors is responsible for activation of Ras-family GTPases. Prog. Nucleic Acid Res. Mol. Biol. **71:**391–444.
43. **Reynolds, L. F., C. de Bettignies, T. Norton, A. Beeser, J. Chernoff, and V. L. Tybulewicz.** 2004. Vav1 transduces T cell receptor signals to the activation of the Ras/ERK pathway via LAT, Sos, and RasGRP1. J. Biol. Chem. **279:**18239–18246.
44. **Roose, J. P., M. Mollenauer, V. A. Gupta, J. Stone, and A. Weiss.** 2005. A diacylglycerol-protein kinase C-RasGRP1 pathway directs Ras activation upon antigen receptor stimulation of T cells. Mol. Cell. Biol. **25:**4426–4441.
45. **Roose, J. P., M. Mollenauer, M. Ho, T. Kurosaki, and A. Weiss.** 2007. Unusual interplay of two types of Ras activators, RasGRP and SOS, establishes sensitive and robust Ras activation in lymphocytes. Mol. Cell. Biol. **27:**2732–2745.
46. **Scheffzek, K., M. R. Ahmadian, and A. Wittinghofer.** 1998. GTPase-activating proteins: helping hands to complement an active site. Trends Biochem. Sci. **23:**257–262.
47. **Schuebel, K. E., X. R. Bustelo, D. A. Nielsen, B. J. Song, M. Barbacid, D. Goldman, and I. J. Lee.** 1996. Isolation and characterization of murine vav2, a member of the vav family of proto-oncogenes. Oncogene **13:**363–371.
48. **Shou, C., C. L. Farnsworth, B. G. Neel, and L. A. Feig.** 1992. Molecular cloning of cDNAs encoding a guanine-nucleotide-releasing factor for Ras p21. Nature **358:**351–354.
49. **Tarakhovsky, A., M. Turner, S. Schaal, P. J. Mee, L. P. Duddy, K. Rajewsky, and V. L. Tybulewicz.** 1995. Defective antigen receptor-mediated proliferation of B and T cells in the absence of Vav. Nature **374:**467–470.
50. **Tian, X., T. Gotoh, K. Tsuji, E. H. Lo, S. Huang, and L. A. Feig.** 2004. Developmentally regulated role for Ras-GRFs in coupling NMDA glutamate receptors to Ras, Erk and CREB. EMBO J. **23:**1567–1575.
51. **Tognon, C. E., H. E. Kirk, L. A. Passmore, I. P. Whitehead, C. J. Der, and R. J. Kay.** 1998. Regulation of RasGRP via a phorbol ester-responsive C1 domain. Mol. Cell. Biol. **18:**6995–7008.
52. **Turner, M., P. J. Mee, A. E. Walters, M. E. Quinn, A. L. Mellor, R. Zamoyska, and V. L. Tybulewicz.** 1997. A requirement for the Rho-family GTP exchange factor Vav in positive and negative selection of thymocytes. Immunity **7:**451–460.
53. **van der Eb, A. J., and F. L. Graham.** 1980. Assay of transforming activity of tumor virus DNA. Methods Enzymol. **65:**826–839.
54. **Vicente-Manzanares, M., and F. Sanchez-Madrid.** 2004. Role of the cytoskeleton during leukocyte responses. Nat. Rev. Immunol. **4:**110–122.
55. **Woodrow, M., N. A. Clipstone, and D. Cantrell.** 1993. p21ras and calcineurin synergize to regulate the nuclear factor of activated T cells. J. Exp. Med. **178:**1517–1522.
56. **Wu, J., S. Katzav, and A. Weiss.** 1995. A functional T-cell receptor signaling pathway is required for $p95^{vav}$ activity. Mol. Cell. Biol. **15:**4337–4346.
57. **Zha, Y., R. Marks, A. W. Ho, A. C. Peterson, S. Janardhan, I. Brown, K. Praveen, S. Stang, J. C. Stone, and T. F. Gajewski.** 2006. T cell anergy is reversed by active Ras and is regulated by diacylglycerol kinase-alpha. Nat. Immunol. **7:**1166–1173.
58. **Zhang, R., F. W. Alt, L. Davidson, S. H. Orkin, and W. Swat.** 1995. Defective signalling through the T- and B-cell antigen receptors in lymphoid cells lacking the vav proto-oncogene. Nature **374:**470–473.
59. **Zhang, W., B. J. Irvin, R. P. Trible, R. T. Abraham, and L. E. Samelson.** 1999. Functional analysis of LAT in TCR-mediated signaling pathways using a LAT-deficient Jurkat cell line. Int. Immunol. **11:**943–950.
60. **Zippel, R., M. Balestrini, M. Lomazzi, and E. Sturani.** 2000. Calcium and calmodulin are essential for Ras-GRF1-mediated activation of the Ras pathway by lysophosphatidic acid. Exp. Cell Res. **258:**403–408.
61. **Zugaza, J. L., M. J. Caloca, and X. R. Bustelo.** 2004. Inverted signaling hierarchy between RAS and RAC in T-lymphocytes. Oncogene **23:**5823–5833.
62. **Zugaza, J. L., M. A. Lopez-Lago, M. J. Caloca, M. Dosil, N. Movilla, and X. R. Bustelo.** 2002. Structural determinants for the biological activity of Vav proteins. J. Biol. Chem. **277:**45377–45392.